

VIBRATIONAL RELAXATION
IN HYDROGEN BONDED SYSTEMS

J. DE BLEIJSER

BIBLIOTHEEK

DELAUS LABORATORIA DER R.U.

Wassenaarseweg 76

Postbus 75 - LEIDEN

VIBRATIONAL RELAXATION IN HYDROGEN BONDED SYSTEMS

PROEFSCHRIFT

TER VERKRIJGING VAN DE GRAAD VAN DOCTOR
IN DE WISKUNDE EN NATUURWETENSCHAPPEN
AAN DE RIJKSUNIVERSITEIT TE LEIDEN,
OP GEZAG VAN DE RECTOR MAGNIFICUS
DR. A.E. COHEN, HOGLERAAR IN DE FACULTEIT
DER LETTEREN, VOLGENS BESLUIT VAN HET
COLLEGE VAN DEKANEN TE VERDEDIGEN
OP WOENSDAG 27 NOVEMBER 1974
TE KLOKKE 14.15 UUR

door

JOHAN DE BLEIJSER

geboren te Rotterdam in 1943

PROMOTOR: DR. J.C. LEYTE

STELLINGEN

1. Slechts in incidentele gevallen is I.R. spectroscopie ($200-5000\text{ cm}^{-1}$) een geschikte techniek ter bestudering van moleculaire beweging in vloeistoffen. Vaker zal deze techniek informatie kunnen leveren over intermoleculaire wisselwerking.

P.C.M. van Woerkom, proefschrift Leiden 1974

Dit proefschrift.

2. Het zou interessant zijn een theorie over ruis in aangedreven systemen te construeren met gebruikmaking van de expansie in cumulanten, en deze te vergelijken met het resultaat van de gebruikelijke perturbatieexpansie.

Bernard en Callen, *Rev. Mod. Phys.* 31, 1017 (1959).

3. Stillinger en Rahman geven ten onrechte de voorkeur aan het gebruik van de diëlectrische formule van Harris en Alder. Onder de gebruikte aannamen zou de formule van Onsager een beter verdedigbare keuze zijn geweest.

Stillinger en Rahman, *J. Ch. Ph.* 60, 1545 (1974)

Buckingham, *Proc. Roy. Soc.* 238A, 235 (1957).

4. De gegevens, op grond waarvan Dotson besluit dat 1-(2-aminoethyl)piperazine Cu(II) chloride een vierkante pyramide als structuur heeft zouden even goed kunnen wijzen op een tetragonaal vervormde octaëdrische omringing.

Dotson, *Inorg. Nucl. Chem. Letters* 10, 879 (1974).

5. Het U.V. spectrum op grond waarvan Tannock stelt dat het beschreven extract uit IBV RNA bevat toont hoofdzakelijk de verontreiniging van het preparaat met fenol.

Tannock, *Archiv für die gesamte Virusforschung* 43, 259 (1973).

6. Het is te betreuren dat Ben-Reuven en Zamir bij hun vergelijking van 1^e en 2^e orde correlatietijden niet de 2^e orde correlatietijden die uit kernspin resonantie gevonden zijn betrekken.

Ben-Reuven en Zamir, *J. Ch. Ph.* 55, 475 (1971).

7. De elektrische installatie in woonhuizen dient uitgerust te zijn met aardstroomrelais.

8. Het is ongewenst dat bij de meeste herdershondenrassen kampioenstitels worden toegekend zonder dat de werkkwaliteiten zijn betrokken bij de beoordeling.

J. de Bleijser

Leiden, 27 november 1974

CONTENTS

CHAPTER I	Introduction	1
	Influence of the physical world	2
	Mathematics	3
CHAPTER II	Geometrical Optics	12
	Reflections at low incidence	13
	Effect of reflection on the wave front	14
	Refraction at normal incidence	15
	Dispersion	16
CHAPTER III	Geometrical Optics	17
	Refractive Index	18
	Influence of various conditions	19
	Dispersion of various media	20
	Reflection	21
CHAPTER IV	Theory	22
	Effect of the ether	23
	General Principles	24
	The ether	25
	Calculation of the optical constants	26
	Mathematical Principles	27
	Some general principles of optics	28
	References	29
	Appendix: Geometrical Optics	30
CHAPTER V	Mathematics	31
	Review of the experimental results	32
	Conclusion	33

*Aan mijn ouders
Voor Dingena en Eddy*

1. The first of the two main sections of the report is devoted to a description of the work done during the year.

2. The second section is devoted to a description of the work done during the year.

1911-12

1911-12

The report is divided into two parts. The first part is devoted to a description of the work done during the year. The second part is devoted to a description of the work done during the year.

CONTENTS

CHAPTER I	Introduction	7
	Outline of the present thesis	9
	References	11
CHAPTER II	Experimental Technique	12
	Measurements at low temperature	14
	Effect of reflection on the band shape	17
	Acquisition of numerical data	20
	References	24
CHAPTER III	Experimental Results	25
	Concentration dependence	31
	Temperature dependence	37
	Influence of solvent composition	39
	Influence of some cations	41
	Influence of some other compounds	42
	References	43
CHAPTER IV	Theory	44
	Outline of the theory	46
	General formalism	49
	The model	53
	Calculation of the dipole moment autocorrelation function	58
	Some remarks concerning convergence	70
	References	73
	Appendix: Numerical integrations	74
CHAPTER V	Discussion	83
	Discussion of the experimental results	86
	Conclusion	89

SAMENVATTING

CONTENTS

1	Introduction	CHAPTER I
2	Outline of the present thesis	
11	References	
12	Experimental technique	CHAPTER II
14	Measurement of low temperatures	
15	Effect of variations on the test setup	
20	Calculation of moment of inertia	
24	References	
25	Experimental results	CHAPTER III
26	The torsion dependence	
27	Temperature dependence	
28	Influence of defect composition	
31	Influence of grain structure	
32	Influence of test speed	
33	References	
34	Theory	CHAPTER IV
35	Outline of the theory	
39	Linear torsion	
41	The model	
42	Calculation of the linear moment	
44	Assumptions for the	
45	Non-linear torsion	
47	References	
48	Appendix: Torsion of rectangular bars	
51	Discussion	CHAPTER V
52	Discussion of the experimental results	
54	Conclusions	

CHAPTER I. INTRODUCTION.

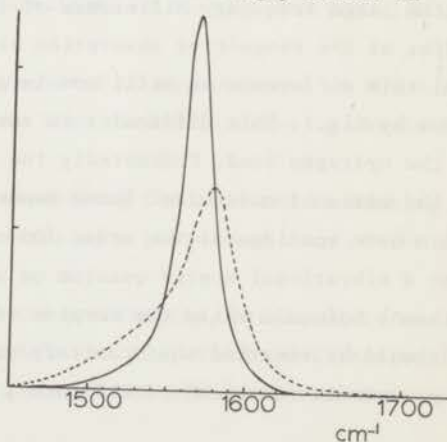
Ever since Infrared Spectroscopy found widespread use, mostly as an analytical tool, it has been used for studying molecular motion and intra- and intermolecular interactions. Especially molecular motion and intermolecular interaction are nowadays the subject of very many spectroscopic studies. It was, however, not before Linear Response Theory (ref.1) had laid a unifying theoretical basis to this work that the potential of I.R. spectroscopy in this respect was fully realised. By the statistical nature of this theory, clearly borne out by the fluctuation-dissipation theorem, it is now clear what is to be expected from each particular branch of spectroscopy.

As will be stated in detail in the theoretical chapter of this thesis it turns out that I.R. spectroscopy can, in favorable cases, supply information concerning certain statistical properties of molecular dynamics and intermolecular interactions.

The present thesis treats a case in which a particular intermolecular interaction can be experimentally suppressed, thereby making it possible to study it separately from the other interactions governing the I.R. spectrum. This decoupling is possible by use of the isotopic dilution method (ref.2).

The principle of this work is shown by discussing some of the experimental findings. Fig.1 shows the asymmetric OCO stretching absorption band of the acetate ion in CH_3OH and CD_3OD . Although the two bands strongly differ in

Fig. 1. Spectrum of the asymmetric OCO stretching band of CH_3COOK in CH_3OH (dotted line) and CD_3OD (solid line)



shape their integrated intensities are the same within experimental error, indicating that both bands represent the same vibrational transition. This suggests some solute-solvent interaction manifest in the solution in CH_3OH but not in CD_3OD . As will be shown in this thesis the effect is caused by near-resonant interaction between the asymmetric OCO stretching oscillators of the acetate ions (at 1570 cm^{-1}) and the COH bending oscillators of CH_3OH (at 1390 cm^{-1}). Isotopic substitution of the solvent removes this latter frequency to much lower wavenumbers, thereby suppressing the effect of this interaction.

The effect of the aforementioned interaction on the band shape may be visualised in the following way.

First it should be noted that when using linear response theory to discuss band shapes it is convenient to discuss the Fourier transform of the band rather than the band itself. This transform, usually denoted the autocorrelation function, decays in time by relaxation processes. If a relaxation process is added that has a rate comparable to the time constant of the autocorrelation function, this latter will decay perceptibly faster. This in turn implies a corresponding broadening of the band.

If now the oscillators under study are coupled to oscillators of comparable frequency via a fluctuating coupling, additional relaxation takes place because an excited oscillator may lose its vibrational energy quantum to a neighbour. If the rate of this process is of the order 0.1 or more psec^{-1} it will broaden the band perceptibly.

Of course vibrational energy transfer has only a significant probability when the interacting oscillators have the same energy level spacings. This condition is not met by the oscillators mentioned above. While the adverse effect of the large frequency difference of 180 cm^{-1} is alleviated by the large widths of the respective absorption bands (which leads to an appreciable overlap) this difference is still too large to account for the considerable effect shown by fig.1. This difficulty is resolved by realising the essential role of the hydrogen bond. Undoubtedly the acetate ions are strongly hydrogen bonded to the methanol molecules. These bonds also have vibrational energy levels which have spacings of the order 100 cm^{-1} (refs.3,4). One can readily imagine that a vibrational energy quantum on an acetate ion can be transferred to a methanol molecule while the surplus energy is taken up by the hydrogen bond. It should be remarked that contrary to resonant vibrational energy transfer (e.g. between identical oscillators), which only causes phase relaxation, in

this case part of the quantum is degraded to thermal energy.

For the sake of clarity the idea behind the present work has been treated extremely loosely. In the theoretical chapter of this thesis it will be treated far more rigorously, at the cost of some conceptual clarity. Therefore this qualitative introduction is considered useful, even if the link with the more rigorous treatment will not always be obvious.

OUTLINE OF THE PRESENT THESIS.

Following this introduction Chapter II treats some details of the experimental technique. While the spectra have been obtained from standard transmittance measurements it is considered useful to discuss those aspects of the technique that deviate from normal I.R. practice. The most important of these is the use of cells with pathlengths in the range of some microns.

In this connection the possible influence of reflection on the measured band shape is discussed.

Chapter II also treats in some detail the system used to record the transmittance spectra numerically. This procedure is necessary to obtain a sufficient number of data points for the Fourier transformation. Measuring the necessary number of points (400 or more) by hand is prohibitively time-consuming.

The experimental results are reported in Chapter III. This chapter consists of two parts, the first of which identifies experimentally the interaction causing the broadening of the as. OCO stretching band of CH_3COOK in CH_3OH with respect to the solution in CD_3OD . It is shown to be a coupling between the as. OCO stretching normal coördinate of the acetate ion with the COH bending of the solvent.

In the second part the results are presented of measurements in which experimentally controllable parameters have been varied in order to obtain information concerning the interaction.

In Chapter IV a theory is developed expressing the measured broadening and shift in terms of the parameters characterising a postulated form of the interaction.

In this theory advantage is taken of the possibility, presented by the cumulant expansion method (ref.5), to single out a specified interaction if the assumption is justified that it is uncorrelated with the other interactions

governing the spectrum. This leads naturally to an expression especially suited to the comparison of the spectra in the case that the interaction is operative and suppressed respectively.

The theory is outlined in the following.

The observed system is described by an ensemble of oscillators, each located on a solute molecule, and interacting with a "bath" at thermal equilibrium. This interaction is considered to cause the oscillators in the ensemble to have a stationary frequency distribution. In this way the concept of inhomogeneous broadening is introduced.

The solute oscillators also interact with an ensemble of solvent oscillators, which likewise has a frequency distribution.

This solvent/solute interaction is written in the simplest possible form taking hydrogen bonding into account. This is an important point, for it will be shown that without the contribution of the hydrogen bond agreement with experiment cannot be obtained.

The interaction is stochastically modulated, mainly because the oscillators are members of ensembles having a frequency distribution, but also by the modulation of the hydrogen bond. This latter modulation is described by a generalised step process which can be interpreted in a variety of ways without the necessity to change the formalism.

The transition dipole moment autocorrelation function, the Fourier transform of which is proportional to the observed absorption band, is then expanded in terms of the solvent/solute interaction. In this procedure the cumulant expansion method is used because this technique has a number of advantages which will be discussed in the theoretical chapter.

The expansion is broken off after the second order. After substitution of the explicit form of the interaction and its modulation the calculation is fairly straightforward. The result is that the ratio of the autocorrelation functions of the bands to be compared is a function of the parameters describing the interaction and the "unperturbed" solvent and solute bands.

From the form of the result it is seen that if the interacting oscillators have widely differing frequencies the interaction has no effect on the band shape. This explains why isotopic substitution of the solvent, which increases this frequency difference by 200 cm^{-1} in the present case, can be used to suppress the effect of this interaction so that it can be studied directly.

Finally, Chapter V compares the experimental results with the theoretical predictions. On the basis of the agreement observed it is concluded that the

theoretical description presented in this thesis is satisfactory. Further work on questions posed by the results is indicated in the last section of this chapter.

References.

1. R. Kubo, J.Ph.Soc.Jap. 12, 570 (1957)
2. P.C.M. van Woerkom, thesis Leiden (1974)
3. P.A. Kollman and L.C. Allen, Chem. Rev. 72, 283 (1972)
4. C. Sandorfy, Can. J. Spect. 17, 24 (1972)
5. R. Kubo, J.Ph.Soc.Jap. 17, 1100 (1962)

CHAPTER II. EXPERIMENTAL TECHNIQUE.

In this chapter attention is given to the technique of the measurements and the acquisition and handling of the numerical data.

While obtaining a spectrum is comparatively straightforward due to the availability of convenient and dependable spectrophotometers the technique of sample preparation is often difficult. Because sample preparation depends strongly on the system to be studied a table is presented here showing some representative experimental systems.

Table 1. Some representative experimental systems.

Sample	Wavenumber interval	Cell pathlength	Window material	Remarks
CH ₃ COOK, 0.1M in CD ₃ OH	1470-1650 cm ⁻¹	0.05 mm (fixed)	CaF ₂	Compensated for solvent absorption.
CH ₃ COOK, 3M in D ₂ O	1470-1650 cm ⁻¹	0.003 mm (fixed)	CaF ₂	Compensated
CH ₃ COOK, 0.1M in CD ₃ OH	1470-1650 cm ⁻¹	0.05 mm (fixed)	NaCl	Compensated Temperature -90°C
CH ₃ OH, pure liquid	1200-1350, 1550-2000 cm ⁻¹	variable around 0.05 mm	Ge	Measurement of refractive index.

Inspection of this table shows first of all that the cell thicknesses are small. Commercial cells are available down to 0.025 mm pathlength, but these have often proved inadequate. In many cases the windows were insufficiently flat or parallel to allow the usual interferometric pathlength determination. Furthermore very thin cells cannot be amalgamated to ensure liquid tightness

because thin spacers immediately dissolve in mercury. Therefore these cells are prone to leak, especially because the temperature in the cell compartment of our spectrophotometer is above ambient. Most fixed pathlength cells were therefore assembled from commercial windows, repolished if necessary, using carefully prepared lead or indium spacers. Especially indium, owing to its ductility, is a very good material for thin spacers. E.g. a cell with a pathlength of a few microns can be made by rolling the indium to a thickness of 0.01 mm with jeweller's rolls, assembling the cell and squeezing it (by trial and error) to the required pathlength. An additional advantage is that such cells are not likely to leak.

A further point borne out by table 1 is that most of the spectra were compensated for solvent absorption. This is accomplished in the usual way by a variable pathlength cell in the reference beam of the spectrophotometer. This cell is adjusted to cancel the solvent absorption, mostly by using a solvent band well removed from the solute band under study. Because it is essential in the present work that the solvents have an absorption band overlapping the solute band this compensation is rather critical. Variable pathlength cells, being essentially hollow micrometers, have the problem of sealing the plunger against the house to prevent leaking whilst still permitting movement of the plunger. This is usually accomplished by a cylindrical Teflon ring mounted on the plunger. By placing this ring under compressive stress it is made to bear on the inside of the cell body. Unfortunately, when this ring is sufficiently compressed to prevent leaking it seriously impedes movement of the plunger. By the accompanying stick-slip the correct compensation is often difficult to obtain.

This problem has been alleviated by fitting the sealing ring with a number of circumferential grooves. These grooves break the capillary action responsible for the leaking and allow a far smaller sealing pressure.

The same type of cell has been used for the last entry of the table. In order to assess the effect of reflection at the interface sample/window on the band shape the refractive index of the solvents was needed. Because great precision is not necessary the refractive index was determined as a function of wavenumber by using a variable pathlength cell as an interferometer. To this end the cell was fitted with germanium windows. After measuring the pathlength by scanning the fringe pattern with air in the cell it was filled with the substance to be measured. Then the desired wavenumber was selected and the pathlength varied as smoothly as possible while

recording the transmittance. From the change of pathlength corresponding to the distance between two adjacent transmittance maxima the refractive index can be calculated. The procedure will be treated in more detail in the following.

This method, though simple in principle, places high demands on the settability and pathlength resolution of the cell. Because these demands are not readily met by the usual 0.5 mm pitch micrometer threads a prototype has been made of a cell design with differential threads of 0.05 mm resultant pitch. Sealing is performed by joining plunger and house with a corrugated nickel membrane. This construction is especially free from the stick-slip and creep inherent in a sliding seal.

The third entry in table 1 is an example of the measurements of the temperature dependence of the band shape.

It is relatively straightforward to cool a sample to temperatures down to -150°C using commercial low temperature cells. In the present study a VLT-2 cell manufactured by RIIC was used. In this design fogging of the windows is prevented by placing the cold cell in a vacuum chamber. While this ensures good thermal insulation it frequently causes the cell to leak. Because in the present work no temperatures lower than -100°C were needed fogging was prevented by flushing the cell jacket with dry nitrogen, the outer windows being omitted.

Compensation for solvent absorption at low temperatures is very difficult. This difficulty arises because variable pathlength cells cannot be cooled. As is to be expected compensation is impossible when the sample cell is cold and the reference cell is at ambient temperature. Therefore compensation was achieved by using two fixed pathlength cells. The reference cell was placed in a second VLT-2 holder. By equipping both cells with indium spacers compensation could be achieved at room temperature by carefully pulling down the cell mounting bolts. In this connection a good deal of feeling is needed to obtain a pair of cells which will behave identically when cooled down to working temperature.

A further point is that CaF_2 windows cannot be used for low temperature work because of their extreme sensitivity to temperature shocks. Therefore NaCl windows were used. Methanol slightly attacks NaCl, destroying the polish, even if it has been previously saturated with NaCl. While this does not impair the measurements it necessitates repolishing if one wants to measure the pathlength interferometrically for a subsequent measurement.

The chemicals

The present study is focused on the spectra of solutions of CH_3COOK and CCl_3COOK in CH_3OH , CD_3OH , CH_3OD , CD_3OD , H_2O and D_2O .

The solvents were of spectroscopic grade (E. Merck, Darmstadt, Uvasol quality) except H_2O and CD_3OH . For H_2O demineralised water was used, and CD_3OH was prepared from CD_3OD (ref 1). CD_3OD was mixed with a fivefold excess of H_2O and distilled slowly. This process was repeated two more times, the last distillation being performed on a spinning band column.

A.R. potassium acetate was dried by melting it in a porcelain crucible until evolution of water vapour ceased. After solidification it was powdered and stored in vacuo in the presence of a phosphorus pentoxide desiccant (Sicapent, E. Merck).

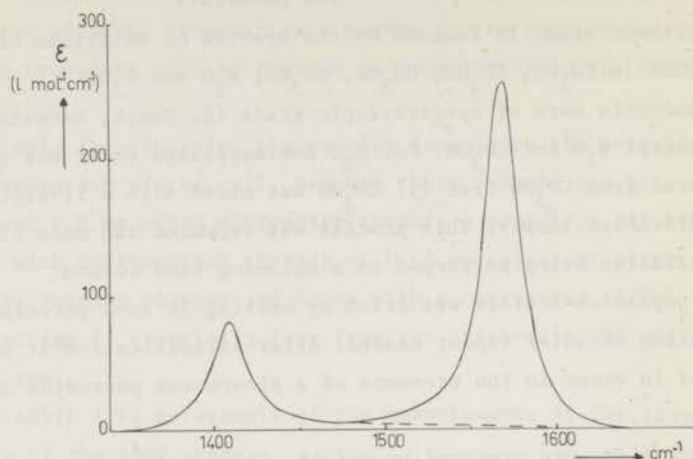
All solutions were prepared by weight. The substances, except of course H_2O , were transferred to the weighing vials in a glove box dried with Sicapent.

The earliest measurements have been performed on a Unicam SP 100 spectrophotometer. This is a double beam, prism/grating, optical null instrument. When this instrument was replaced with a Perkin-Elmer model 325 all previous measurements were repeated on this instrument and checked for consistence. Although the measurements have been performed by three experimenters on two different instruments the agreement is complete. This indicates that the necessary repeatability can be obtained routinely.

The only problem in measuring is the low energy available because the solvent absorbs from 50 to 95% of the incident radiation. This entails measuring times up to several hours which necessitates high stability of the electronics. This stability is most conveniently checked by the flatness of the 0% T line vs. time and vs. wavenumber. The first measurements were problematic because the SP 100 was severely lacking in this respect. With the advent of the PE325 stability could simply be obtained by measuring in a thermostatted room and by flushing the instrument with dry air.

Concerning the spectral resolution no special measures have been taken. The standard slit program provides a resolution better than 1 cm^{-1} . Because the total width of all bands under study exceeds 20 cm^{-1} the standard slit program was used throughout. This implies that the resolution is not constant over the band, but with broad bands it was preferred to fix the energy rather than the resolution.

Fig. 1 Spectrum of the OCO stretching bands of CH_3COOK in CD_3OD .



A complication arises with respect to the analysis of the spectra. This can be seen from fig. 1 which shows the spectrum of the carboxylate stretch of the acetate ion in CD_3OD . The band at 1410 cm^{-1} is the symmetric OCO stretch absorption, and the band at 1570 cm^{-1} is the asymmetric stretch. This latter band is the one studied in most detail in the present work. Unfortunately it is overlapped to some extent by the symmetric stretch band. Any procedure to separate the bands is necessarily arbitrary. In addition such procedures would be useless in this work because in CD_3OH , the most important solvent, the symmetric band cannot be measured with any precision because in this region the solvent absorbs most of the incident energy. Therefore it was considered unavoidable to define the baseline as is shown in fig. 1 by the broken line. While this may seem serious it should be borne in mind that only the low frequency half of the band is affected to some extent, and that the greatest influence is on the wing of the band. Because this latter exerts only minor influence on the time dependence of the Fourier transform of the band (ref. 2) it is considered preferable to accept this small distortion rather than to rely on some separation procedure.

Furthermore Fourier cosine transformation is only sensitive to the part, even in frequency with respect to the origin, which in our case is the band maximum. When the overlap is not too serious this fact tends to reduce the error. Of course the opposite holds for the sine transform, but in the present stage of the work the emphasis is laid on the cosine transform because

this displays most clearly the effect under study, viz. the influence of oscillator/oscillator interaction on vibrational relaxation.

Moreover the aim of this work is not to explain the complete autocorrelation function, or equivalently the complete band shape. Instead the autocorrelation functions of the same band in slightly different solvents but measured in the same way are compared and only their ratio is discussed. Because the measured effect is very large it is assumed that this particular choice of baseline does not appreciably influence the results.

Another point concerning the dependability of the measured band shape is the possible influence of the solute on the solvent band shape. If this shape is greatly altered by the presence of the solute compensation for the solvent absorption will obviously be impossible. Even if one succeeds in setting the reference cell to such a pathlength that a normal-looking spectrum is obtained the measurement is meaningless because it is not known how much of the observed band is to be attributed to the solvent.

Because methanol strongly affects the solute band shape (by oscillator/oscillator interaction, as will be shown by the theory) the solute certainly influences the methanol spectrum. It should however be borne in mind that while in the solution every acetate ion is coupled to methanol, the great majority of the methanol molecules is not coupled to an acetate ion. Therefore the spectral distortion of the solvent is limited to a number of molecules of the same order of magnitude as the number of solute ions. Because the transition dipole moment of the solvent oscillators is smaller by an order of magnitude than that of the solute oscillators the effect of this distortion is considered to be negligible. The effect of the presence of spectroscopically inert ions has been found to be negligible also.

Effect of reflection on the band shape.

The intensity of the light transmitted by a sample depends not only on the transmittance of the sample proper but also on reflection and interference. These two effects depend on the complex refractive index $\hat{n} = n - iK$ of the sample and therefore on the frequency. It is known that problems arise when the imaginary part K of the sample refractive index is larger than 0.2 and the cell pathlength consequently below 10 microns. Because in the present work pathlengths in this range have been used occasionally it was considered desirable to estimate the effect of reflection in these cases.

When the optical constants of the windows and sample and the pathlength are known it is possible to calculate this effect (refs. 2,3) but the calculations are tedious. Compared to the examples treated in ref. 3 two aspects of our work warrant an approximate treatment. In the first place the values of K in the present work never fall in the range where dramatic effects occur, viz. when K is of the order 1. The second point is that the samples in this work, being dilute solutions, do not show such strong variations of the real part of the refractive index as are found in pure liquids when $K_{\max} \approx 1$. In the latter case n may vary from 0.6 through 3 over a band.

Furthermore the measurements show no evidence of interference. This is inferred from the fact that the band shape for a given sample is independent of the pathlength. (Of course the pathlength can only be varied by a factor of 2 because otherwise photometric errors predominate.)

Therefore it was considered sufficient to calculate the reflectivity R of the interface sample/window as a function of frequency. Denoting the window refractive index by n_w and the complex refractive index of the sample by $\hat{n} = n - iK$ the reflectivity is given (for normal incidence) by:

$$R = \frac{(n - n_w)^2 + K^2}{(n + n_w)^2 + K^2}$$

It is assumed that if the quantity $(1 - R)^2$, or for compensated measurements $(1 - R_{\text{sample}})^2 / (1 - R_{\text{reference}})^2$, is not frequency dependent by more than 0.5% the measurement can be considered to yield a dependable band shape.

A model calculation on a hypothetical sample, made by combining the optical constants of the 1640 cm^{-1} band of H_2O with those of the 1470 cm^{-1} band of solid Na_2CO_3 (ref. 4) in various proportions, has shown that no significant band shape distortions are to be expected for the measurements in this work.

Because the frequency dependence of R is most pronounced in regions where the solvent refractive index changes steeply with frequency it was considered necessary to measure the refractive index of the solvents used in this work over the frequency range of the solute band.

These measurements have been performed by using a variable pathlength cell as a Fabry-Perot interferometer. To this end a variable pathlength cell (RIIC type XLO) was fitted with germanium windows. To check the mechanical stability the fringe pattern was scanned directly after assembly and an hour later, first with air in the cell and again after the cell had been filled with the sample. When this check was satisfactory the cell was emptied and dried.

Then the scale of the cell was calibrated in the pathlength range to be used. This is done by scanning the fringe pattern at fixed wavenumber by slowly diminishing the pathlength. From the position of the maxima the correction factor is found. Then the cell is filled with the sample and adjusted to a pathlength corresponding to a maximum. At fixed wavenumber the cell is slowly closed again while the number of transmittance maxima encountered is counted. This process is stopped when a maximum near the end of the pathlength range is reached. From the pathlength difference corresponding to the distance between two adjacent maxima the refractive index can then be calculated.

The results for H_2O and CH_3OH are shown in fig. 2.

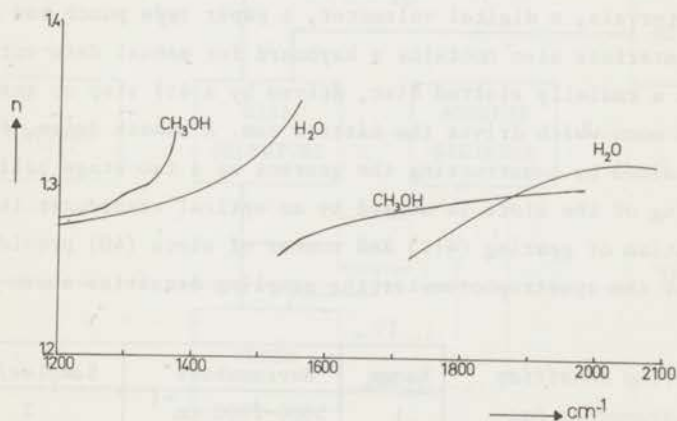


Fig. 2 Refractive index of H_2O and CH_3OH .

Acquisition of numerical data.

Because the present study is focused on dipole autocorrelation functions the transmittance spectra have to be converted to extinction spectra and subsequently subjected to Fourier transformation. This operation, which in practice can only be performed by computer, necessitates at least 400 data points (i.e. transmittance values) for each band. As the labor to measure so many points by hand and to punch them on cards is prohibitive the spectrophotometer was equipped with a digital data acquisition system. Such systems are available commercially, but because they are expensive our system was made in the laboratory.

The system consists of a pulser, triggering the digitising sequence at fixed wavenumber intervals, a digital voltmeter, a paper tape punch and an interface unit. The interface also contains a keyboard for manual data entry.

The pulser is a radially slotted disc, driven by a 4:1 step up gearbox from the shaft of the worm which drives the Littrow cam. A smooth drive, free from backlash, is obtained by constructing the gearbox as a two stage ball chain drive. The passing of the slots is sensed by an optical transducer (Leuze LS 03). The combination of gearing (4:1) and number of slots (40) provides on the various ranges of the spectrophotometer the sampling densities shown in table 2.

Table 2. Sampling densities on the four wavenumber ranges of the spectrophotometer.

Range	Wavenumbers	Samples/cm ⁻¹
1	5000-2000 cm ⁻¹	2
2	2500-1000 cm ⁻¹	4
3	1000-400 cm ⁻¹	10
4	450-200 cm ⁻¹	20

The spectrophotometer is equipped with a slave potentiometer providing a voltage proportional to the transmittance value. By sampling this voltage at fixed wavenumber intervals the need to record the wavenumber of each data point is obviated. Digitising of the transmittance values is performed by a digital voltmeter (Solartron LM 1450). On receipt of a sample command it takes a sample of this voltage, converts it to digital form and presents it via a fan out unit (Solartron EX 1613) in parallel BCD format. The digital output is held until the next sample command. By the interface unit these data, having a digital resolution of 1 in 2000, are routed to a paper tape punch (Facit 4070). The mode of operation of the system will be sketched with reference to its block diagram (fig. 3).

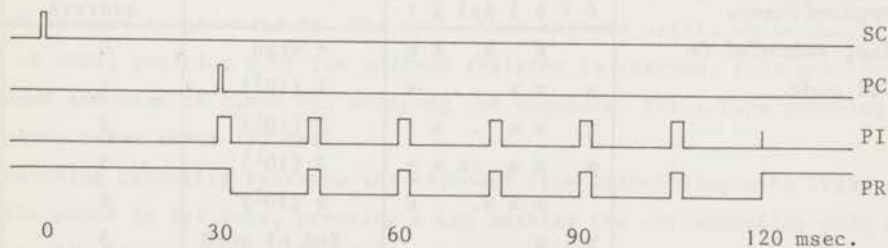
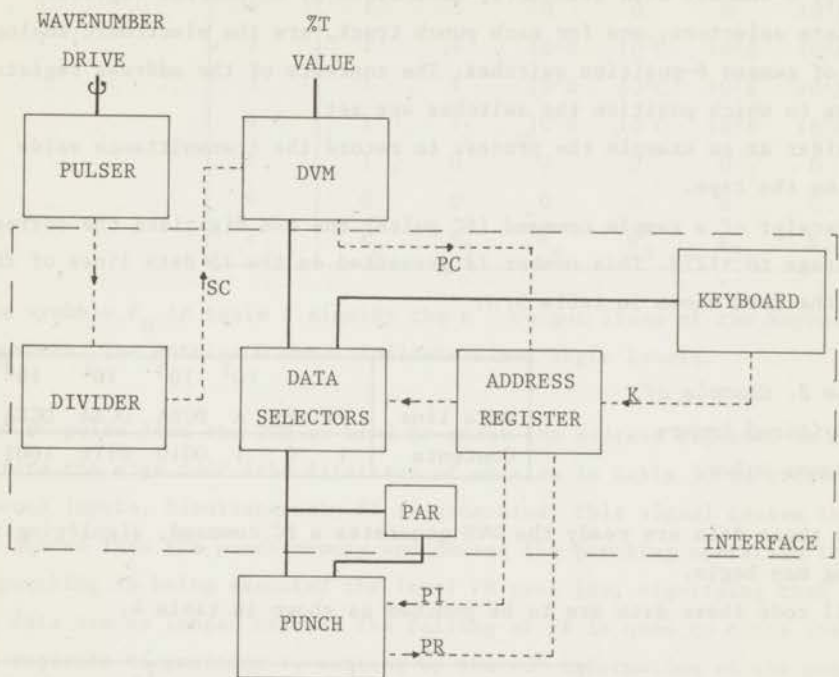


Fig. 3 Block diagram of the digital data acquisition system and timing sequence of the punch interface.

Heavy lines: data routing.

Dotted lines: control functions.

Remark: The pulse widths in the timing sequence are not to scale.

The main function of the interface unit is to reformat the parallel BCD data to ASCII code. In this code each transmittance value occupies 6 rows on the tape viz. sign, thousands, hundreds, tens, units, space. The required parallel to serial conversion and character generation are performed by 8-channel data selectors, controlled by an address register. These data selectors, one for each punch track, are the electronic analog of a bank of ganged 8-position switches. The contents of the address register determines to which position the switches are set.

Consider as an example the process to record the transmittance value 0.6395 on the tape.

On receipt of a sample command (SC pulse) the DVM digitises the corresponding voltage to +1279. This number is presented on the 15 data lines of the DVM in the form shown in table 3.

Table 3. Example of a digitised transmittance value.

Data line	10^3		10^2		10^1		10^0	
	P+	P-	A	DCBA	DCBA	DCBA	DCBA	
Contents	1	0	1	0010	0111	1001		

When these data are ready the DVM generates a PC command, signifying that punching may begin.

In ASCII code these data are to be punched as shown in table 4.

Table 4. Example of a transmittance value, recorded in ASCII code.

Track no.	Meaning	Data selector address
8 7 6 5 4s3 2 1		
x x . x x	+ sign	0
x x x . x	1 (10^3)	1
x x x . x	2 (10^2)	2
x x x . x x x	7 (10^1)	3
x x x . x	9 (10^0)	4
x x .	End of word	5

In track s the sprocket holes are punched. Because track 7 is never used for the symbols generated by the DVM and by the keyboard this track is not equipped with a data selector. Track 8 is controlled by a parity generator and therefore also has no selector.

To generate the appropriate codes the 6 data selectors are wired according to table 5.

Table 5. Wiring
of the data
selector inputs.

Input no.	Data selector no.					
	6	5	4	3	2	1
0	1	0	1	P-	P+	1
1	1	1	0	0	0	10 ³ A
2	1	1	10 ² D	10 ² C	10 ² B	10 ² A
3	1	1	10 ¹ D	10 ¹ C	10 ¹ B	10 ¹ A
4	1	1	10 ⁰ D	10 ⁰ C	10 ⁰ B	10 ⁰ A
5	1	0	0	0	0	0
6	0	0	0	0	0	0
7	K ₆	K ₅	K ₄	K ₃	K ₂	K ₁

The symbols K_n in table 5 signify the n^{th} output lines of the keyboard code matrix. The entries 0 and 1 indicate fixed logic levels.

The PC pulse from the DVM is used to reset the address register to 0. Therefore the sign code (the first row of entries in table 5) is presented to the punch inputs. Simultaneously PI is generated. This signal causes the data to be loaded into the punch memory and causes the punching operation to begin. When punching is being executed the level PR goes low, signifying that the input data are no longer needed. The falling of PR is used to clock the address register to position 1, setting up the 10³ information on the punch inputs. When the punching of the sign code is completed PR goes high again, which is made to generate PI. The cycle then repeats until, while punching End of Word, position 6 of the address register is reached. This position is decoded and used to block PI, stopping the sequence. The entire punching sequence takes about 120 msec.

Latching circuitry prevents the keyboard from interfering with this process. If the punch is not busy, pressing a key enables the corresponding code matrix lines. Simultaneously a pulse K is generated which presets the address register to position 7 and generates PI. This causes the contents of the code matrix line to be punched. The subsequent rising of PR is used now to inhibit PI, so that the keyboard entry is punched only once.

A parity generator connected to the 6 active data lines controls track 8 to obtain even parity.

From table 2 it is seen that in the ranges 3 and 4 the number of samples per wavenumber can be excessive. Therefore a divider is provided enabling one

to divide this number by any number from 1 through 99.

An electromechanical counter registers the total number of transmittance values recorded.

The interface unit was implemented with standard TTL circuits. The actual procedure to calculate the Fourier transforms, including a discussion of the reliability, has been treated in detail in ref. 2.

The program used was written by H. S. Kielman and subsequently elaborated by J. J. Joolen.

References.

1. Beersmans and Jungers, Bull. Soc. Chim. Belg. 56 72 (1947)
2. P.C.M. van Woerkom, Thesis Leiden (1974)
3. R.D. Young and R.N. Jones, Chem. Rev. 71 219 (1971)
4. Poe-Ju Wu, Thesis University of Virginia (1967)

CHAPTER III. EXPERIMENTAL RESULTS.

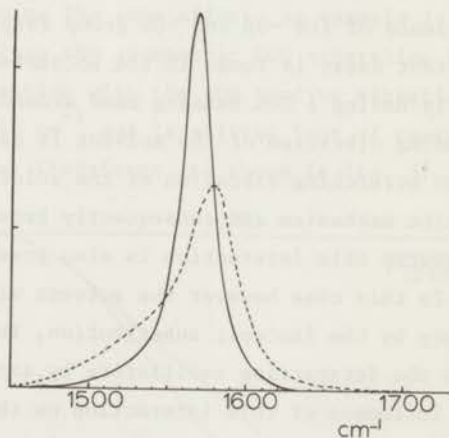
This chapter is divided into two parts. In the first part the effect studied in this thesis and presented already in the introductory chapter is discussed more fully. The interaction held responsible for the effect is treated in some detail and additional experimental evidence supporting the proposal is presented and discussed.

In the second part of this chapter the experimental results of a systematic study of the properties of the interaction are presented.

Part I.

Fig. 1 shows again the marked difference in band shape of the asymmetric OCO stretching band of acetate ions in CH_3OH compared to CD_3OD as the solvent.

Fig. 1. Spectrum of the asymmetric OCO stretching vibration of CH_3COOK in CH_3OH (broken line) and in CD_3OD (solid line). Absorbance scale is the same for both bands but in arbitrary units.

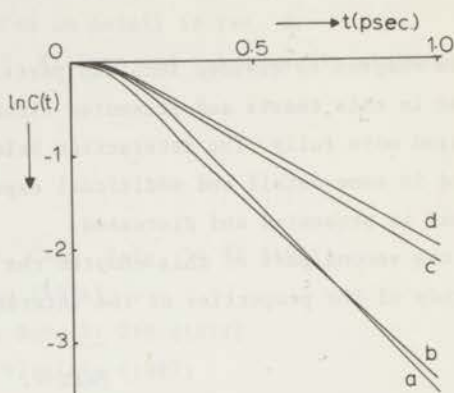


The broadening observed in CH_3OH is suggestive of some specific solvent/solute interaction, manifest in the solution in CH_3OH but not in that in CD_3OD . In connection with this idea it is significant that CH_3OH has a broad absorption band on the low frequency side of the solute band and partially overlapping the latter. This solvent band, situated at 1400 cm^{-1} , does not correspond to a single vibrational transition however.

In order to determine which solvent vibrational mode gives rise to the observed broadening the spectra, or rather the corresponding Fourier cosine transforms, of the asymmetric OCO stretching band of the acetate ion in CH_3OH , CH_3OD , CD_3OH and CD_3OD have been determined. These transforms are shown in fig. 2.

Fig. 2. Electric moment auto-correlation functions of the as. OCO stretching band of CH_3COOK in:

- a) CH_3OH
- b) CD_3OH
- c) CH_3OD
- d) CD_3OD



These functions are immediately seen to form two groups, characterised by the presence of the -OH and -OD group respectively in the solvent molecules. The fastest decay is found in the solvents possessing an -OH group and consequently having a COH bending band around 1400 cm^{-1} . From this result the COH bending vibration of the solvent is assumed to interact with the asymmetric OCO stretching vibration of the solute, giving rise to an additional relaxation mechanism and consequently broadening the solute band.

Of course this interaction is also present in the solutions in CH_3OD and CD_3OD . In this case however the solvent vibration is shifted to much lower frequency by the isotopic substitution, increasing the frequency difference between the interacting oscillators by about 200 cm^{-1} (ref. 1). This suppresses the influence of this interaction on the relaxation.

The interaction provides a relaxation mechanism because it is subject to stochastic modulation. For a discussion of the resonant character of this mechanism it is convenient to visualise it as intermolecular vibrational energy transfer.

It is obvious that coupled oscillators having the same (unperturbed) frequencies can exchange vibrational energy quanta. If the interaction were constant a quantum would just oscillate back and forth, but in an ensemble of

such pairs in which the coupling is stochastically modulated this exchange leads to relaxation.

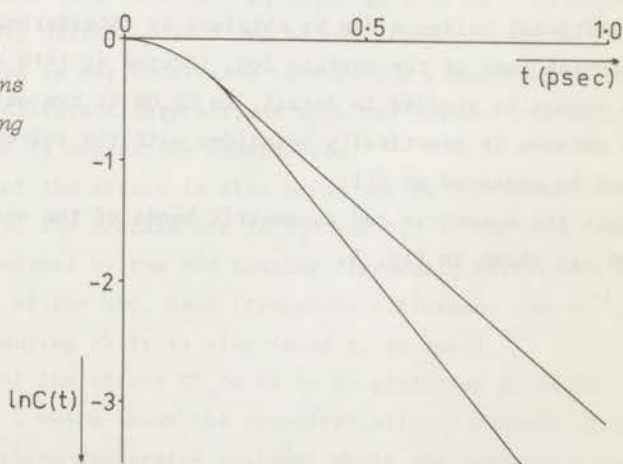
It is also obvious that the probability of energy transfer will decrease sharply when the oscillators differ in frequency. As long as the Fourier spectrum of the modulation of the interaction bridges the frequency gap the probability of energy transfer will be significant.

In the present case (acetate ions in CD_3OH) the average frequencies of the solvent and solute oscillators differ by 180 cm^{-1} and the overlap of the bands is relatively minor. The consequence of this situation is that the probability of energy transfer is small unless a large interaction energy with a wide modulation spectrum is assumed. It has been calculated however that such a strong interaction would give rise to a much larger shift than is actually observed.

This problem is solved by realising that a smaller interaction is necessary if the spectrum of its modulation has a maximum at a frequency approximately corresponding to the frequency difference between the interacting oscillators. It will be shown in the present thesis that the hydrogen bond provides an interaction of the required form.

Other systems have been found showing the same effect. An example is the acetate ion in H_2O and D_2O . In this case the asymmetric OCO stretching band of the acetate is broadened by interaction with the HOH bending vibration of H_2O . This vibration is located at 1640 cm^{-1} and is shifted "out of reach" by deuteration. The corresponding Fourier transforms are shown in fig. 3.

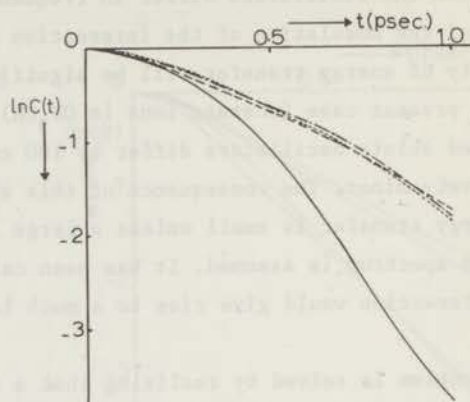
Fig. 3. Electric moment autocorrelation functions of the as. OCO stretching band of CH_3COOK in H_2O (lower curve) and D_2O (upper curve).



The resonant nature of the effect is demonstrated again by the spectra of the CCl_3COO^- ion in CH_3OH , CD_3OD , H_2O and D_2O . The autocorrelation functions calculated from these measurements are shown in fig. 4.

Fig. 4. Electric moment autocorrelation functions of the as. OCO stretching band of CCl_3COOK in:

- : CH_3OH
- - - - - : CD_3OD
- : H_2O
- - - - - : D_2O



By the substitution of Cl for H the as. OCO stretch of the ion is shifted to 1680 cm^{-1} . The frequency difference with the COH bending vibration of CH_3OH is now seen to be so large that the interaction has no more effect in CH_3OH than it has in CD_3OD . On the other hand the results in H_2O and D_2O are as expected by the interaction with the HOH bending vibration at 1640 cm^{-1} . The agreement between the autocorrelation functions in CH_3OH and CD_3OD on the one hand and those in D_2O on the other is considered to be fortuitous.

Additional evidence can be obtained by considering the symmetric OCO stretching band of the acetate ion, located at 1410 cm^{-1} . Unfortunately this band cannot be studied in detail. In CD_3OH it can only be observed qualitatively because it practically coincides with the solvent band, and in CH_3OH it cannot be measured at all.

Both the symmetric and asymmetric bands of the acetate ion in CD_3OH and CD_3OD are shown in fig. 5.

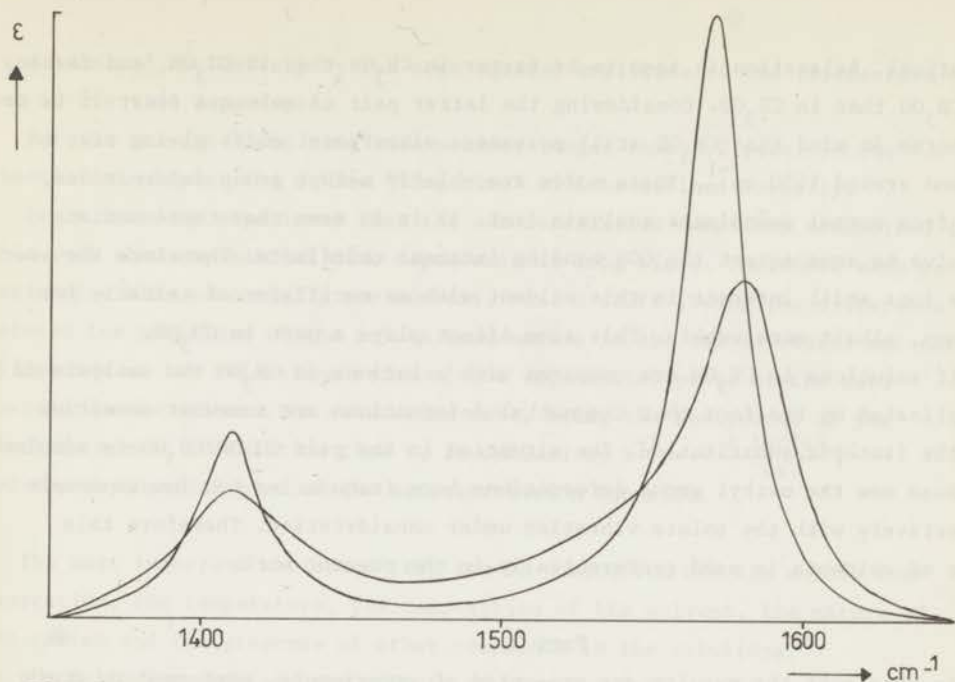


Fig. 5. Spectra of the OCO stretching bands of CH_3COOK in CD_3OH and CD_3OD .
By inspection two points are evident.

The first is that contrary to the asymmetric band the symmetric one is not shifted. As will be shown by the theory this is to be expected because for the symmetric vibration the frequency difference with the solvent vibration is negligibly small.

The second point is that it is broadened to a greater extent than the as. band. The latter is broadened from 22.5 cm^{-1} in CD_3OD to 37.5 cm^{-1} in CD_3OH , while the sym. band has half widths of 24.5 and 62 cm^{-1} respectively in these solvents. While this finding is not conclusive because the respective normal modes will generally have different interactions with the solvent vibration the magnitude of the effect is suggestive nonetheless.

The resonant character of the effect is also borne out by the symmetric band. Comparing solutions of the acetate ion in H_2O and D_2O it is found that in H_2O the as. band is broadened by the HOH bending (frequency difference 80 cm^{-1}) while the broadening of the sym. band (frequency difference 230 cm^{-1}) is only slight. The accompanying shift is also found to be small.

For a systematic study of the effect CD_3OH is to be preferred to CH_3OH . This may be seen from fig. 2 which shows the autocorrelation functions of the as. band in CH_3OH and its three deuterated analogs. While the autocorrelation functions form two groups the functions within each group are clearly not

identical. Relaxation is seen to be faster in CH_3OH than in CD_3OH , and faster in CH_3OD than in CD_3OD . Considering the latter pair of solvents first it is to be borne in mind that CH_3OD still possesses vibrational modes giving rise to a band around 1400 cm^{-1} . These modes are chiefly methyl group deformations, but from normal coördinate analysis (ref. 1) it is seen that these motions involve to some extent the COD bending internal coördinate. Therefore the acetate ions still interact in this solvent with an oscillator of suitable frequency, albeit more weakly. This same effect plays a part in CH_3OH .

If solutions in CH_3OH are compared with solutions in CH_3OD the analysis is complicated by the fact that the methyl deformations are somewhat sensitive to the isotopic substitution. The situation in the pair $\text{CD}_3\text{OH}/\text{CD}_3\text{OD}$ is simpler because now the methyl group deformations have frequencies too low to couple effectively with the solute vibration under consideration. Therefore this pair of solvents is used preferentially in the present work.

Part 2.

In this part the results are presented of experiments, performed to study the effect of oscillator/oscillator interaction on the band shape and the factors influencing this effect.

For each experiment, which consists of comparing the solute band shapes in two related solvents, the obtainable data are the positions of the solute band maxima and the respective band shapes.

Actually the Fourier cosine transforms of the bands are compared rather than the bands themselves. In the present study the long time behaviour of these transforms is considered. There are two reasons for this choice, the first of which is of a practical nature. It has been shown by van Woerkom (ref. 2) that, contrary to the prevailing opinion, the time dependence of an experimental autocorrelation function at long times can be determined far more precisely than that at short times.

The second reason is that the long time behaviour of the autocorrelation function can be expressed in terms of quantities characterising the interaction and its modulation. In the theoretical chapter it will become apparent that in the present case the long time behaviour yields more information than the dependence on short times. This may be anticipated by considering the usual technique to study the short time part of the autocorrelation function, viz. fitting a Gaussian to it for small times. In the case that the relaxation is caused by a modulated interaction, as it is in this work, the Gaussian part

is determined exclusively by the mean squared amplitude of the interaction and not by its time dependence.

For the present "long time" means times longer than 0.2 psec. In the theoretical chapter the notion "long time" will be defined formally.

It is found by experiment that the autocorrelation functions determined in this work show exponential time dependence at long times. Therefore each experiment yields essentially two numbers, viz. a shift (being the difference between the positions of the solute band maxima in the two solvents) and the difference of the relaxation rates of the exponential parts of the autocorrelation functions. The relaxation rate, being the reciprocal of the electric moment correlation time τ , is defined by $\tau^{-1} = - \frac{d \ln C(t)}{dt}$ for the exponential part of the autocorrelation function.

The most important variables that can be controlled are the solute concentration, the temperature, the composition of the solvent, the nature of the cation and the presence of other compounds in the solutions. In the following sections the effects of these variables will be presented.

1. Concentration dependence of the correlation time.

For the as. OCO stretching absorption band of acetate ions the dependence of τ^{-1} on the acetate concentration has been determined in CH_3OH , CD_3OH , CD_3OD , H_2O and D_2O .

The results of the measurements, performed on CH_3COOK as the solute, are summarised in tables 1 through 5 and figs. 6 through 11.

Table 1. Concentration dependence of the correlation time of the as. OCO stretching band of CH_3COOK in CH_3OH .

Conc. (mole/l)	Pathlength (microns)	Integrated Intensity ($\text{l.mole}^{-1}.\text{cm}^{-2}$)	σ_{max} (cm^{-1})	$\Delta\sigma_{\frac{1}{2}}$ (cm^{-1})	τ^{-1} (psec^{-1})
0.098	30.6	26,500	1581	41.0	4.39
0.198	26.6	32,300	1581	42.5	4.39
0.304	23.0	28,700	1581	42.0	4.39
0.503	13.4	30,500	1580	42.2	4.39
1.02	7.7	28,000	1582	42.5	4.39
1.64	6.5	28,300	1582	43.2	4.39
1.96	5.5	25,400	1582	43.5	4.39

Fig. 6. Electric moment autocorrelation functions of the as. OCO stretching band of CH_3COOK in CH_3OH . Upper curve: 0.098 mole/l Lower curve: all curves for concentrations from 0.2 to 2 mole/l.

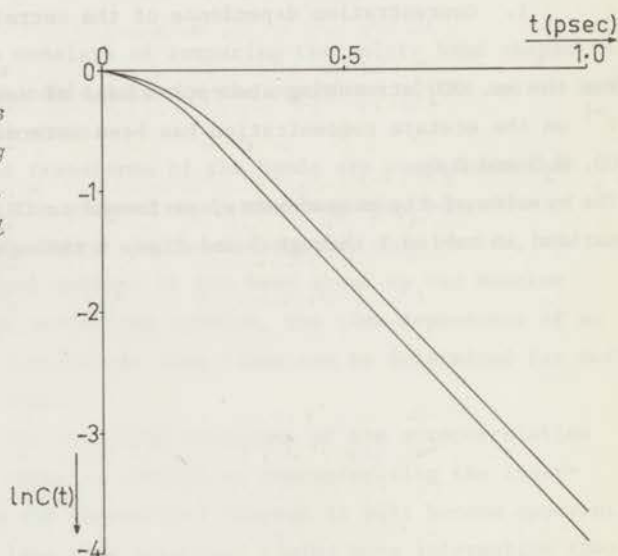


Table 2. Concentration dependence of the correlation time of the as. OCO stretching band of CH_3COOK in CD_3OH .

Conc. (mole/l)	Pathlength (microns)	Integrated Intensity ($\text{l.mole}^{-1}.\text{cm}^{-2}$)	σ_{max} (cm^{-1})	$\Delta\sigma_{\frac{1}{2}}$ (cm^{-1})	τ^{-1} (psec^{-1})
0.22	40.8	28,800	1579.5	38.6	3.78
0.53	13.9	34,000	1580	39.8	3.78
0.93	8.2	30,000	1580	38.5	3.78
2.09	4.5	26,100	1583	38.0	3.78

Fig. 7. Electric moment autocorrelation function of the as. OCO stretching band of CH_3COOK in CD_3OH . Over a concentration range from 0.2 to 2 mole/l all curves coincide.

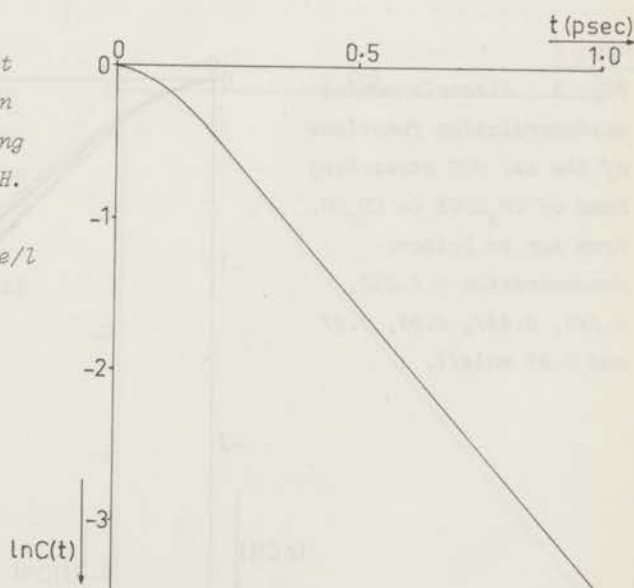


Table 3. Concentration dependence of the correlation time of the as. OCO stretching band of CH_3COOK in CD_3OD .

Conc. (mole/l)	Pathlength (microns)	Integrated Intensity ($1.\text{mole}^{-1}.\text{cm}^{-2}$)	σ_{max} (cm^{-1})	$\Delta\sigma_{\frac{1}{2}}$ (cm^{-1})	τ^{-1} (psec^{-1})
0.050	99.7	36,900	1570	23.1	2.07
0.148	31.2	37,200	1570	23.1	2.15
0.497	11.5	37,100	1570	23.7	2.30
0.98	3.2	39,100	1571	25.4	2.42
1.97	1.6	42,900	1572	28.4	2.92
1.97	2.6	42,400	1572	28.0	2.84

Fig. 8. Electric moment autocorrelation functions of the as. OCO stretching band of CH_3COOK in CD_3OD . From top to bottom: Concentration = 0.050, 0.148, 0.497, 0.98, 1.97 and 1.97 mole/l.

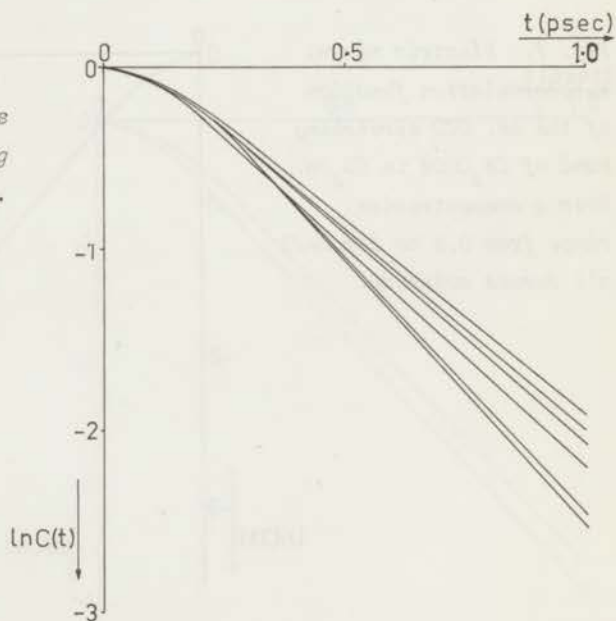


Table 4. Concentration dependence of the correlation time of the as. OCO stretching band of CH_3COOK in H_2O .

Conc. (mole/l)	Pathlength (microns)	Integrated Intensity ($\text{l.mole}^{-1}.\text{cm}^{-2}$)	σ_{max} (cm^{-1})	$\Delta\sigma_{\frac{1}{2}}$ (cm^{-1})	τ^{-1} (psec^{-1})
0.288	13.4	26,900	1554	45.7	4.90
0.397	12.6	22,500	1554	46	4.90
0.507	14.6	30,700	1554	49	4.90
0.507	9.9	30,800	1554	52	4.90
0.992	9.8	22,700	1554	47.5	4.90

Fig. 9. Electric moment autocorrelation function of the as. OCO stretching band of CH_3COOK in H_2O . Over a concentration range from 0.288 to 0.992 mole/l all curves coincide.

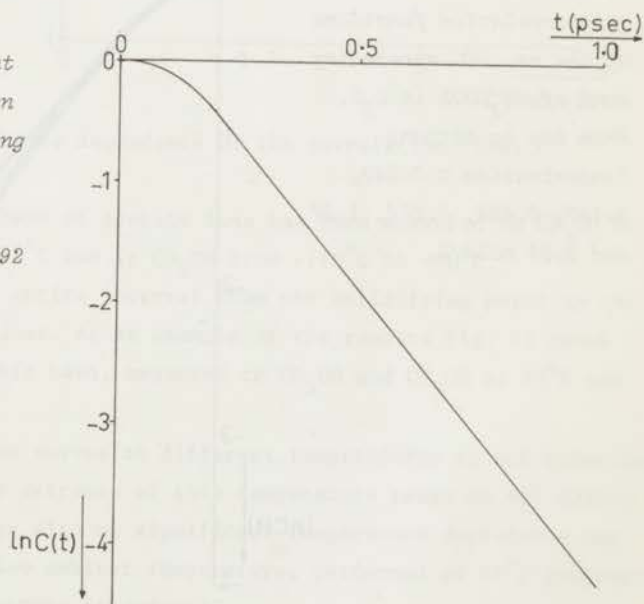
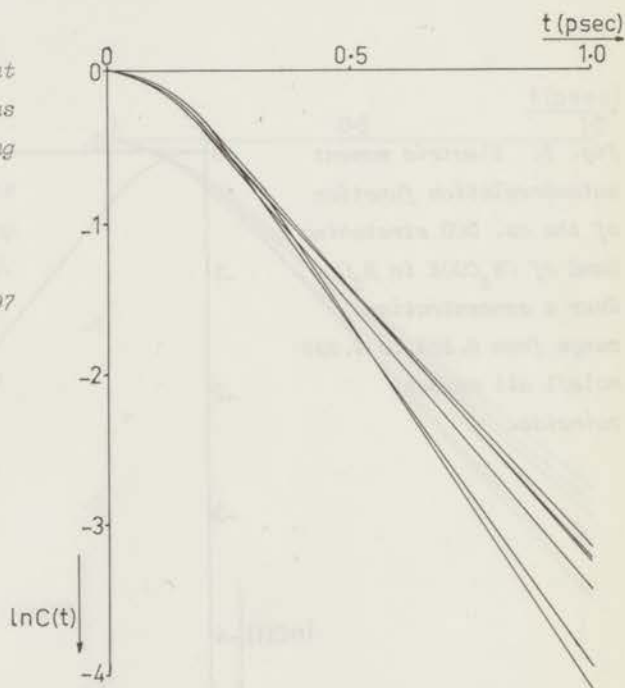


Table 5. Concentration dependence of the correlation time of the as. OCO stretching band of CH_3COOK in D_2O .

Conc. (mole/l)	Pathlength (microns)	Integrated Intensity ($\text{l.mole}^{-1}.\text{cm}^{-2}$)	σ_{max} (cm^{-1})	$\Delta\sigma_{\frac{1}{2}}$ (cm^{-1})	τ^{-1} (psec^{-1})
0.049	149	31,700	1560.6	37.0	3.56
0.150	49.5	32,800	1561.1	35.5	3.54
0.603	18.7	32,400	1561.0	36.0	3.62
0.974	12.1	29,200	1562.5	38.4	3.76
1.97	3.8	33,900	1562.4	40.1	4.30
2.95	2.9	27,900	1561.5	41.7	4.60
2.95	2.7	27,400	1562.1	41.0	4.80

Fig. 10. Electric moment autocorrelation functions of the as. OCO stretching band of CH_3COOK in D_2O . From top to bottom: Concentration = 0.049, 0.150, 0.603, 0.974, 1.97 and 2.95 mole/l.



It is immediately seen that tables 1, 2 and 4 and figs. 6, 7 and 9 do not show any measurable concentration dependence of the correlation time. On the other hand tables 3 and 5 and figs. 8 and 10 show a linear increase of the reciprocal of the correlation time with solute concentration. This is especially clearly brought out by fig. 11.

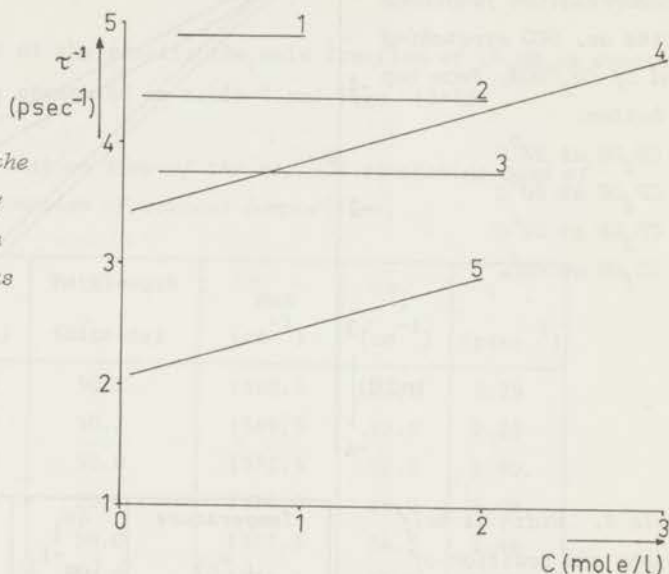


Fig. 11. τ^{-1} of the as. OCO stretching band of CH_3COOK in various solvents as a function of the concentration.

- 1) H_2O
- 2) CH_3OH
- 3) CD_3OH
- 4) D_2O
- 5) CD_3OD

2. Temperature dependence of the correlation time.

The as. OCO stretching band of acetate ions has been measured in CD_3OD at temperatures from 23°C to 60°C and in CD_3OH from -110°C to $+60^\circ\text{C}$. The latter range spans the entire interval from the solidifying point to the boiling point of the solutions. As an example of the results fig. 12 shows the cosine transforms of this band, measured in CD_3OH and CD_3OD at 23°C and 60°C .

It is seen that while the curves at different temperatures do not coincide the correlation time at the extremes of this temperature range do not differ measurably. Within the range also no significant temperature dependence was found. The measurements below ambient temperature, performed at 10°C intervals likewise did show no temperature dependence.

The main parameters (position and width) of the solute band are shown in table 6. While the band shape shows some broadening around the maximum when the temperature is lowered its position and half width are seen to change only

little. Over the temperature range of table 6 the solute band remains at 1575 cm^{-1} with the same shape.



Table 6. Width at half height and position of the COH bending band of CD_3OH as a function of temperature.

Temperature ($^\circ\text{C}$)	$\Delta\sigma_{\frac{1}{2}}$ (cm^{-1})	σ_{max} (cm^{-1})
+24	122	1397
0	118	1400
-20	118	1402
-40	117	1406
-60	118	1410
-80	118	1416
-100	120	1415

From these results it is concluded that the temperature dependence of the correlation time of the band under consideration is at most very slight.

As a practical point this is convenient because it obviates the necessity to measure in thermostatted cells.

3. Influence of the solvent composition on the correlation time.

The correlation time of the as. OCO stretching band of CH_3COOK has been measured in $\text{CD}_3\text{OH}/\text{CD}_3\text{OD}$ mixtures as a function of the composition of the solvent.

In the presentation of the results the mole fraction of CD_3OH is denoted by x_H . The results are presented in table 7 and figs. 13-15.

Table 7. Correlation time of the as. OCO stretching band of CH_3COOK as a function of solvent composition.

x_H	Conc. (mole/l)	Pathlength (microns)	σ_{max} (cm^{-1})	$\Delta\sigma_{\frac{1}{2}}$ (cm^{-1})	τ^{-1} (psec^{-1})
0.0	0.099	50.2	1569.5	23.3	2.29
0.0	0.099	50.2	1569.5	23.9	2.25
0.251	0.100	50.0	1572.5	27.3	2.80
0.514	0.120	50.4	1574.0	31.0	3.08
0.760	0.135	50.0	1577.3	34.5	3.46
0.760	0.135	50.0	1576.7	35.0	3.50
1.000	0.106	74.2	1579.2	37.0	3.64

Fig. 13. Electric moment autocorrelation functions of the as. OCO stretching band of CH_3COOK in $\text{CD}_3\text{OH}/\text{CD}_3\text{OD}$ mixtures. From top to bottom:

- $x_H = 0.000$
- $x_H = 0.251$
- $x_H = 0.514$
- $x_H = 0.760$
- $x_H = 1.000$

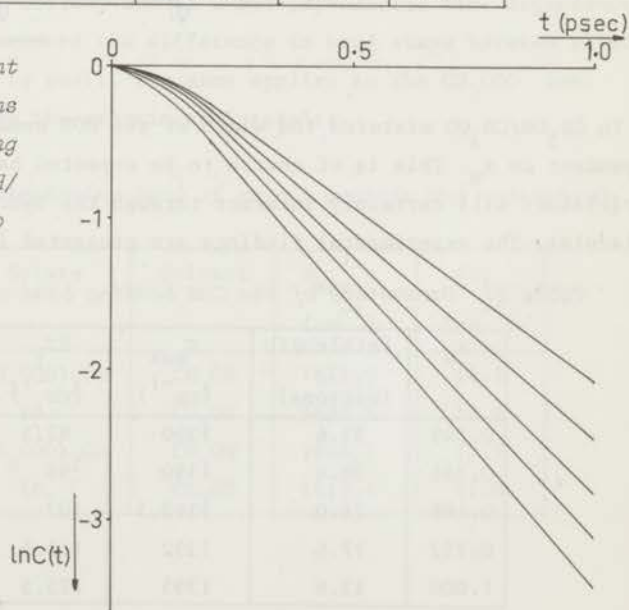


Fig. 14. τ^{-1} of the as. OCO stretching band of CH_3COOK in $\text{CD}_3\text{OH}/\text{CD}_3\text{OD}$ mixtures as a function of solvent composition.

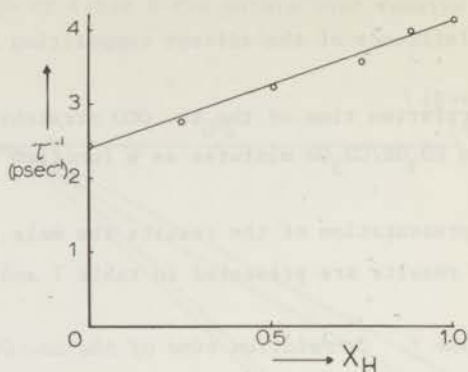
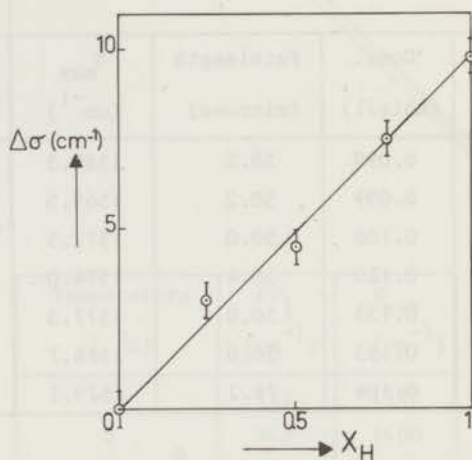


Fig. 15. Shift of the as. OCO stretching band of CH_3COOK in $\text{CD}_3\text{OH}/\text{CD}_3\text{OD}$ mixtures as a function of solvent composition. The shift is defined with respect to the band position in CD_3OD .

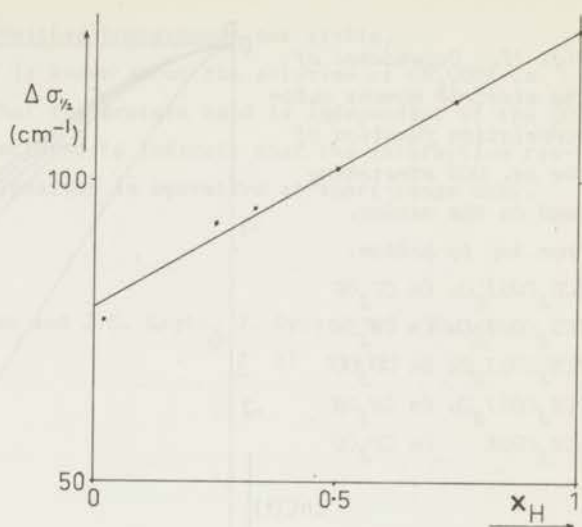


In $\text{CD}_3\text{OH}/\text{CD}_3\text{OD}$ mixtures the width of the COH bending band is found to be dependent on x_H . This is of course to be expected because the COH bending oscillators will certainly interact through the hydrogen bonds coupling the molecules. The experimental findings are presented in table 8 and fig. 16.

Table 8. Parameters of the COH bending band of CD_3OH as a function of x_H

x_H	Pathlength (microns)	σ_{max} (cm^{-1})	$\Delta\sigma_{\frac{1}{2}}$ (cm^{-1})	Integrated Intensity
0.249	53.6	1390	92.5	2060
0.344	38.4	1390	96	2060
0.468	26.0	1390.5	102	2040
0.752	17.6	1392	113.5	1960
1.000	13.6	1395	125.5	2160

Fig. 16. Half width of the COH bending band of CD_3OH in CD_3OD as a function of x_H .



4. Influence of some cations on the correlation time.

It has been found that there is little or no difference if Na^+ or Li^+ is substituted for K^+ as the cation.

On the other hand the cupric ion has a profound influence. The as. OCO stretching band is shifted to 1626 cm^{-1} and it is narrowed to a half width of 14 cm^{-1} . The corresponding autocorrelation function decays much slower than in the case that K^+ is the cation, and it shows exponential time dependence only after 1.5 psec. Furthermore the difference in band shape between solutions in CH_3OH and in CD_3OD is small. The same applies to the CD_3COO^- ion.

Table 9 and fig. 17 show the experimental results.

Table 9. The as. OCO stretching band of cupric acetate and -acetate- D_3 .

Conc. (mole/l)	Solute	Solvent	σ_{\max} (cm^{-1})	$\Delta\sigma_{1/2}$ (cm^{-1})
0.036	$(CH_3COO)_2Cu$	CH_3OH	1626.5	14.2
0.037	id.	CD_3OD	1625.6	13.6
0.036	$(CD_3COO)_2Cu$	CH_3OH	1616.7	12.7
0.036	id.	CD_3OD	1615.4	11.8

Fig. 17. Dependence of the electric moment auto-correlation function of the as. OCO stretching band on the cation.

From top to bottom:

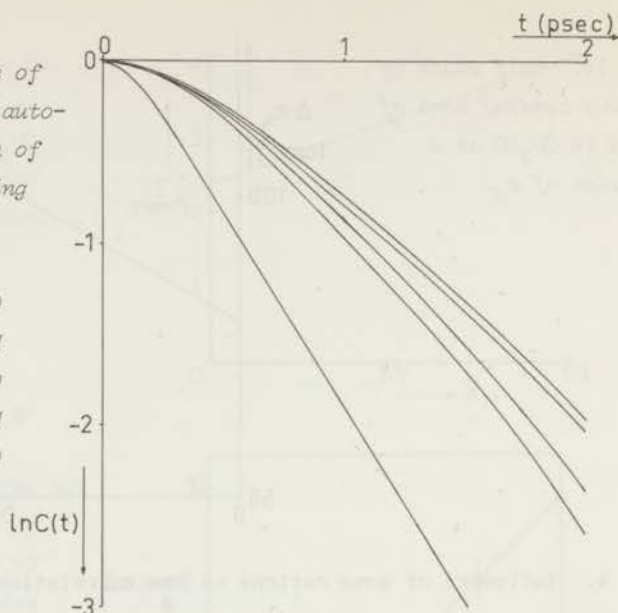
$(CD_3COO)_2Cu$ in CD_3OD

$(CD_3COO)_2Cu$ in CH_3OH

$(CH_3COO)_2Cu$ in CD_3OD

$(CH_3COO)_2Cu$ in CH_3OH

CH_3COOK in CD_3OD



It should be remarked that in order to obtain a clear solution about 0.035 M acetic acid had to be added. Concerning the addition of acetic acid it has been found that relaxation in lithium acetate solutions is faster in the presence of acetic acid in the solutions, and that also the concentration dependence is affected. This is however the subject of further study and will not be treated in the present work.

5. Influence of the presence of other compounds in the solutions.

In order to find a possible effect of spectroscopically inert ions on the band shape solutions of CH_3COOK in CD_3OD and D_2O were saturated with KBr . This did not produce any measurable change of the solute band shape.

Solutions of CH_3COOK in CH_3OH have been mixed with CCl_4 . This gives clear solutions irrespective of the ratio CH_3OH/CCl_4 . It is found that the shape of the as. OCO stretching band of the acetate ion is completely independent of the presence of CCl_4 . Therefore it is thought that methanol cannot be displaced from the "solvation sphere" of the acetate by the apolar CCl_4 .

It is however not known how large the "solvation complexes" are if they exist at all, because it is possible that the solution is not really homogeneous or indefinitely stable. It has e.g. been found that sodium acetate, dissolved in methanol, can be mixed with CCl_4 giving a clear solution but

that the resulting mixture is neither homogeneous nor stable.

As long as nothing definite is known about the solution of CH_3COOK in $\text{CH}_3\text{OH}/\text{CCl}_4$ mixtures the fact that the acetate band is independent of the CCl_4 concentration can only be conjectured to indicate that the interaction responsible for the additional relaxation is operative at short range only.

Reference.

1. H.M.R. Arbouw-van der Veen and J.C. Leyte, *J. Cryst. Mol. Struct.*

2 17 (1972)

CHAPTER IV. THEORY.

INTRODUCTION.

In this chapter a theoretical analysis is presented of the influence of intermolecular interaction on the shape of an I.R. absorption band. In line with the principle, expressed in the fluctuation-dissipation theorem, that relaxation is connected with fluctuation it will become apparent that broadening is not caused by the interaction as such but by the modulation of the interaction.

Apart from inhomogeneous broadening and irrespective of the modulation mechanism a frequency band of width $\Delta\omega$ is produced by modulation of the central frequency by processes with lifetimes of the order $(\Delta\omega)^{-1}$. Typical I.R. bands for which inhomogeneous broadening is not predominant have a width of the order of 10 cm^{-1} , corresponding to modulation frequencies up to 2 rad.psec^{-1} . Processes influencing I.R. bands therefore have lifetimes on a picosecond scale. This implies that the fastest single process to which an I.R. band is sensitive is short time molecular dynamics. In some cases fast vibrational relaxation by intermolecular vibrational energy transfer has been shown to have a comparable influence (ref. 1).

Consider now the case that a frequency band is caused by a number of modulation processes, each of which can be switched off at will. By comparing bands with a particular modulation on and off each process can be studied by its effect. However, maximum detail can only be observed for a process whose Fourier spectrum has its maximum in the neighbourhood of $\Delta\omega$. This does not imply that slower processes, i.e. processes having maximum spectral density at a frequency $\ll \Delta\omega$ cannot be observed. For a process to appreciably influence a band it is only necessary that the process has a nonnegligible spectral density around $\Delta\omega$.

Consider e.g. an interaction $X(t)$ moving in discrete steps around a zero average. In a second order treatment its effect will be governed by the auto-correlation function $\langle X(0).X(t) \rangle$. For many processes this function has the

form: $\langle X(0) \cdot X(t) \rangle = \langle X^2 \rangle \cdot e^{-\lambda t}$

λ is the rate of the steps, $\langle X^2 \rangle$ is the variance of the magnitude X .

The corresponding spectral density is given by:

$$J(\omega) = \int_{-\infty}^{\infty} dt e^{i\omega t} \langle X(0) \cdot X(t) \rangle = 2 \langle X^2 \rangle \frac{\lambda}{\lambda^2 + \omega^2} = 2 \langle X^2 \rangle \cdot \frac{\lambda^{-1}}{1 + (\lambda^{-1} \omega)^2}$$

For frequencies much larger than the rate of the steps, i.e. when $\lambda^{-1} \omega \gg 1$, the spectral density is seen to decrease with the square of the frequency. However it increases with the variance. Therefore the influence of this process on a band of width $\Delta\omega \gg \lambda$ can be appreciable if the variance is sufficiently large.

In ref.1 a number of systems has been treated for which the band widths are to a large degree determined by vibrational relaxation. It should be remarked that in these systems one observes predominantly phase relaxation. In such a case the vibrational quanta are not, either partly or wholly, degraded to thermal energy but only exchanged between identical oscillators.

The systems studied in ref.1 are all simple, weakly associated liquids. Such liquids are characterised by relatively narrow absorption bands and do not contain other modes with energies in the neighbourhood of the vibration under study and coupled sufficiently to it to provide a relaxation mechanism.

The systems treated in the present thesis differ from those in ref.1 in two essential ways.

First, the "unperturbed" absorption band of the sample is not a delta function but a band of considerable width which is caused by inhomogeneous broadening. This means that the reference state of the system is a state in which otherwise identical oscillators have different energies. This spread in energies is caused by slow but strong modulation processes. In this context strong means nonnegligible with respect to kT .

The second difference is that the additional broadening is caused by interaction between oscillators with different energies. This implies that if one considers vibrational energy transfer to be a relaxation mechanism some energy will have to be transferred to or from the thermal bath.

This chapter treats the essential role of the hydrogen bond in this process. Furthermore it will become apparent that the complicated nature of the systems studied precludes assignment of one single mechanism to the observed relaxation.

OUTLINE OF THE THEORY.

For convenience an outline of the theory developed in this chapter is presented here.

The starting point is the linear response theory as presented e.g. in ref.3. The main reason for choosing this theory is that it relates the response of a macroscopic system to an externally applied perturbation to equilibrium properties of the system. These are just what one is usually interested in.

In optical spectroscopy the external disturbance is formed by the electromagnetic field of the light, and the response of the system is governed by its electric dipole moment operator. The motion of this operator under the equilibrium Hamiltonian of the system determines the frequency dependent admittance tensor of the system. Usually the imaginary part of this tensor is measured spectroscopically and its frequency dependence is compared with predictions of the theory concerning the system that one wants to test.

From such comparisons parameters characterising statistical properties of the system may be obtained. It has been found possible e.g. to obtain data on rotational diffusion in some cases, while also interaction between the transition dipole moments of some molecular vibrations has been observed (ref.1 and references therein).

From linear response theory it is found that the problem consists in calculating the dipole moment autocorrelation function. This function has the form:

$$\text{Tr } \rho [\vec{M}, \vec{M}(t)]_+ ; \quad \rho \text{ being the density operator}$$

It is seen to depend on the motion of the electric moment operator \vec{M} under the Hamiltonian of the system.

The aim of the present theory is to assess the influence of a specified interoscillator interaction on this motion. To this end the Hamiltonian is split into four parts. The first part describes the intermolecular vibrations with energy level spacings $\gg kT$. One species from this set is experimentally observed and is therefore separately considered together with the vibration with which it is supposed to interact.

The second part consists of all other degrees of freedom and is called the bath. It modulates the intramolecular oscillators and the interaction between them. The third part consists of all interactions coupling the oscillators to each other and to the bath, except the interaction which we propose to study. This interaction forms the fourth part of the Hamiltonian.

The first and second terms of the Hamiltonian are denoted by $\hbar E$ and $\hbar F$ respectively, and the third and fourth are for the moment together denoted by $\hbar G$. Then the autocorrelation function can be written:

$$\text{Tr } \rho [\vec{M}, \vec{M}(t)]_+ = \text{Tr } \rho [\vec{M}, e^{i(E+F+G)t} \vec{M} e^{-i(E+F+G)t}]_+$$

Separating the exponential operators in the standard way gives:

$$\begin{aligned} \text{Tr } \rho [\vec{M}, \vec{M}(t)]_+ &= \text{Tr } \rho [\vec{M}, \exp_0 \left\{ i \int_0^t dt' \overline{\overline{G}}(t') \right\} \vec{M}(t) \exp_0 \left\{ -i \int_0^t dt' \overline{\overline{G}}(t') \right\}]_+ = \\ &= \text{Tr } \rho [\vec{M}, \exp_0 \left\{ i \int_0^t dt' \overline{\overline{G}}^{\times}(t') \right\} \vec{M}(t)]_+ \end{aligned}$$

The double bar indicates the interaction representation under $\hbar E$ and $\hbar F$. Written in this way this expression can be regarded as a special form of average of the exponential operator $\exp_0 \left\{ i \int_0^t dt' \overline{\overline{G}}^{\times}(t') \right\}$. This enables us to expand the autocorrelation function using the cumulant expansion technique (ref.5). This technique is chosen for its good convergence properties. In order to apply this the average has to be normalised in which connection it is remarked that the normalising function is itself time dependent.

The cumulant expansion is carried to second order. The properties of cumulants enable us to separate the interaction under study from all other interactions by assuming it to be uncorrelated (in the special sense of the particular averaging procedure) with the other interactions. Then a mathematical form is chosen for this interaction and the cumulants are calculated by standard quantummechanical means.

The key assumption in the calculation is that the spectrum of $\hbar E$ in the region of interest is a band, caused by a stationary distribution of frequencies. The term "stationary" is to be referred here to the time scale characteristic of the autocorrelation function, which is of the order of 1 psec. Aside from the influence on the way in which the averages are calculated the main effect of this assumption is that it takes into account all interactions governing the band shape (except of course the interaction under study) without the need to postulate a detailed model for them.

The final result of the calculation shows clearly the resonant character

of the interaction, i.e. the interaction has only an appreciable effect between oscillators with approximately equal frequencies. Alternatively oscillators with different frequencies can only interact to some effect when the frequency gap is bridged by an oscillatory component in the interaction, such as can be provided by a hydrogen bond. The results show that this last effect can be very important.

The resonant character of the interaction is the reason that this interaction can be observed experimentally. By increasing the frequency gap through isotopic substitution of the oscillators the effect of the interaction is suppressed.

In the present study the system is a dilute solution, and the observed oscillators are located on the solute molecules. They interact with oscillators on the solvent molecules. Therefore the experiment consists in comparing the solute spectra in the normal and isotopically substituted solvent respectively.

The theory is especially suited to such experiments because it concentrates on the effect of a specified interaction on a band, the shape of which is not of primary interest but is instead regarded as an experimental datum. Actually the theory is found to express the ratio of the Fourier transforms of the two experimental band shapes (this ratio being a function of time) in terms of the parameters describing the interaction and its motion.

GENERAL FORMALISM

The general formalism used here has already been presented (refs.1,2). For convenience it will be treated briefly here.

Because infrared spectroscopy measures the frequency dependent response of a macroscopic system to a (electromagnetic) perturbation it is natural to use the linear response theory (ref.3) as a starting point. This theory expresses the dissipative part $\chi''(\omega)$ of the admittance tensor in terms of the time evolution of the electric moment operator \vec{M} of the system.

$$\chi''(\omega) = \frac{\omega}{4E_{\beta}(\omega)} \int_{-\infty}^{\infty} dt e^{-i\omega t} \text{Tr } \rho [\vec{M}, \vec{M}(t)]_+$$

As usual for isotropic systems only the zz component will be treated

$$\chi''_{zz}(\omega) = \frac{\omega}{4E_{\beta}(\omega)} \int_{-\infty}^{\infty} dt e^{-i\omega t} \text{Tr } \rho [M_z, M_z(t)]_+ \quad E_{\beta}(\omega) = \frac{1}{2} \hbar \omega \coth \frac{1}{2} \beta \omega \quad (1)$$

$$\beta \equiv \hbar/kT$$

At the frequencies of interest ($\sigma > 1000 \text{ cm}^{-1}$) $\omega/E_{\beta}(\omega)$ is insensitive to ω and can therefore be assumed constant over absorption bands of not too large width. In this case the Fourier transform of $\chi''_{zz}(\omega)$, which is available experimentally, is proportional to the autocorrelation function $\phi_{zz}(t)$ defined by: $\phi_{zz}(t) = \frac{1}{2} \text{Tr } \rho [M_z, M_z(t)]_+$ (2)

In this expression the electric moment operator \vec{M} moves under the complete Hamiltonian $\hbar H$ of the macroscopic sample, which may be written:

$$\hbar H = \hbar(E^{\circ} + F + G^{\circ})$$

$\hbar E^{\circ}$ is the Hamiltonian of all intramolecular vibrational degrees of freedom of the isolated molecules, in so far as the corresponding energies are $\gg kT$. These degrees of freedom are denoted by "the system".

$\hbar F$, the bath Hamiltonian, contains all other degrees of freedom.

$\hbar G^{\circ}$ is the interaction Hamiltonian coupling the intramolecular vibrational degrees of freedom to each other and to the bath.

Due to the large magnitude of the interaction a perturbation treatment in terms of $\hbar G^{\circ}$ is impracticable. Therefore the Hamiltonian is redefined by inclusion of the bath average of $\hbar G^{\circ}$ in the vibrational Hamiltonian and sub-

traction of the same quantity from $\hbar G^0$:

$$E = E^0 + \text{Tr}^F \rho G^0 \quad G = G^0 - \text{Tr}^F \rho G^0$$

$$\hbar H = \hbar(E^0 + F + G^0) = \hbar(E + F + G)$$

A second argument for this redefinition is the following. The interaction is an energy fluctuating around a large average value. Only the fluctuation causes the relaxation that is the subject of the present study. Therefore it is not worthwhile to carry the average through the calculation where it would only cause problems without contribution to the desired information.

Under the assumption that the fluctuation $\hbar G$ is small the density operator ρ will be approximated by:

$$\rho = \frac{e^{-\beta H}}{\text{Tr} e^{-\beta H}} \approx \frac{e^{-\beta(E+F)}}{\text{Tr} e^{-\beta(E+F)}} \quad (5)$$

Because evidently $[E, F]_- = 0$ it is now possible to average over vibrational and bath coördinates separately.

By use of the notation $A^X B = [A, B]_-$ and the identity $e^{A^X} \cdot B = e^A B e^{-A}$ (ref.3) we may write $M_z(t)$ in the form:

$$M_z(t) = e^{i(E+F+G) \times t} M_z = \exp_0 \left\{ i \int_0^t dt' \overline{G}^X(t') \right\} \overline{M}_z(t) \quad (6)$$

The symbol \exp_0 denotes a time ordered exponential, i.e. an exponential in the expansion of which the operators have to be ordered according to a certain prescription concerning their time arguments. In the present case the time ordering is such that the time arguments increase to the right.

This ordering may be verified by directly calculating this expansion by use of the well-known integral equation for the time evolution operator $U(t)$.

Defining $\hbar H = \hbar(H_0 + V)$, $U(t) = U_0(t) \cdot U_V(t) = \exp(-iH_0 t) \cdot U_V(t)$ and $\overline{V}(t) = U_0^\dagger(t) \cdot V \cdot U_0(t)$ this equation has the form:

$$U(t) = U_0(t) \cdot U_V(t) = U_0(t) \cdot \left\{ 1 - i \int_0^t dt' \overline{V}(t') \cdot U_V(t') \right\}$$

Iteration leads to the series solution:

$$U(t) = U_0(t) \cdot \sum_0^{\infty} (-i)^n \int_0^t dt' \dots \int_0^{t^{(n-1)}} dt^{(n)} \overline{V}(t') \cdot \overline{V}(t'') \dots \overline{V}(t^{(n)})$$

in which the time arguments are seen to decrease to the right. Because the expansion of the exponent in eq.6 leads to the series for $U_V^\dagger(t)$ the time

arguments in eq.6 are seen to increase to the right.

$$\bar{M}_Z(t) \text{ is defined by: } \bar{M}_Z(t) \equiv e^{iE^X t} \bar{M}_Z(t) \equiv e^{iE^X t} e^{iF^X t} M_Z \quad (7)$$

Using eq.6 $\phi_{ZZ}(t)$ can be written:

$$\phi_{ZZ}(t) = \frac{1}{2} \text{Tr } \rho [M_Z, \exp_0 \left\{ i \int_0^t dt' \bar{G}^X(t') \right\} \bar{M}_Z(t)]_+ \quad (8)$$

$\bar{M}_Z(t)$ is now written in a spectral resolution using an eigenbasis of $\hbar E$.

$$\bar{M}_Z(t) = \sum_{\alpha} \bar{M}_Z^{\alpha}(t) e^{i\alpha t} \quad (9)$$

The frequency components $\bar{M}_Z^{\alpha}(t)$ of $\bar{M}_Z(t)$ still move, but only under $\hbar F$.

Because the I.R. spectrum is studied in a frequency range containing only one absorption band the resulting $\phi_{ZZ}^{\alpha}(t)$ is the component of $\phi_{ZZ}(t)$ determined by the components $\bar{M}_Z^{\pm\alpha}(t)$ if the band under study is sufficiently isolated from the rest of the spectrum (ref.4).

Therefore we can write:

$$\phi_{ZZ}^{\alpha}(t) = \frac{1}{2} \text{Tr } \rho [M_Z^{-\alpha}, \exp_0 \left\{ i \int_0^t dt' \bar{G}^X(t') \right\} \bar{M}_Z^{\alpha}(t)]_+ \cdot e^{i\alpha t} \quad (10)$$

A convenient method to treat this expression is the cumulant expansion technique (ref.5). In order to apply this the quantity to be expanded has to be written in the form of a dimensionless average. To obtain this form we define:

$$\phi_{ZZ}^{\alpha,0}(t) = \frac{1}{2} \text{Tr } \rho [M_Z^{-\alpha}, \bar{M}_Z^{\alpha}(t)]_+ \cdot e^{i\alpha t} \quad (11)$$

and write, using this as a normalising function:

$$\begin{aligned} \phi_{ZZ}^{\alpha}(t) &= \phi_{ZZ}^{\alpha,0}(t) \frac{\text{Tr } \rho [M_Z^{-\alpha}, \exp_0 \left\{ i \int_0^t dt' \bar{G}^X(t') \right\} \bar{M}_Z^{\alpha}(t)]_+}{\text{Tr } \rho [M_Z^{-\alpha}, \bar{M}_Z^{\alpha}(t)]_+} \\ &\equiv \phi_{ZZ}^{\alpha,0}(t) \cdot \left\langle\left\langle \exp_0 \left\{ i \int_0^t dt' \bar{G}^X(t') \right\} \right\rangle\right\rangle \end{aligned} \quad (12)$$

The average denoted by the double brackets and defined by eq.(12) is seen to fulfill the condition that $\left\langle\left\langle 1 \right\rangle\right\rangle = 1$, which is necessary for the cumulant expansion theorem to apply (ref.5). The result of this expansion is to second order

$$\phi_{zz}^{\alpha}(t) = \phi_{zz}^{\alpha,0}(t) \cdot \exp\left\{i \int_0^t dt' \left\langle\left\langle \bar{G}^x(t) \right\rangle\right\rangle_c - \int_0^t dt' \int_0^{t'} dt'' \left\langle\left\langle \bar{G}^x(t'') \bar{G}^x(t') \right\rangle\right\rangle_c\right\} \quad (13)$$

In general $\hbar G$ includes different kinds of interaction, e.g. interactions of one oscillator with the bath and interoscillator interactions. Denoting these by $\hbar G_1$ and $\hbar G_2$ respectively we make the assumption that mixed cumulants vanish, i.e. $\hbar G_1$ and $\hbar G_2$ are assumed to be uncorrelated in the sense of the definition (12). Then $\phi_{zz}^{\alpha}(t)$ can be written

$$\begin{aligned} \phi_{zz}^{\alpha}(t) &= \phi_{zz}^{\alpha,0}(t) \cdot \exp\left\{i \int_0^t dt' \left\langle\left\langle \bar{G}_1^x(t') \right\rangle\right\rangle_c - \int_0^t dt' \int_0^{t'} dt'' \left\langle\left\langle \bar{G}_1^x(t'') \bar{G}_1^x(t') \right\rangle\right\rangle_c\right\} \cdot \\ &\quad \cdot \exp\left\{i \int_0^t dt' \left\langle\left\langle \bar{G}_2^x(t') \right\rangle\right\rangle_c - \int_0^t dt' \int_0^{t'} dt'' \left\langle\left\langle \bar{G}_2^x(t'') \bar{G}_2^x(t') \right\rangle\right\rangle_c\right\} \\ &= \phi_{zz}^{\alpha,0}(t) \cdot F_1(t) \cdot F_2(t) \end{aligned} \quad (14)$$

If it is possible experimentally to suppress the effect of the interoscillator interaction on $\phi_{zz}^{\alpha}(t)$ it is possible in principle to compare the expression $F_2(t)$ with experiment.

Because it is intuitively clear that interoscillator interaction will depend on the energy matching between the oscillators it is a reasonable hypothesis that isotopic dilution may suppress this interaction. Under this assumption the theory is developed in the present form. From the final form of (14) this hypothesis will readily be verified.

THE MODEL

In order to apply the formalism to a specific problem the spectrum of $\hbar E$, the explicit form of $\hbar G$ and a model for the motions under the bath Hamiltonian are needed. These points are the subject of this section.

Because the system as defined below eq.3 consists exclusively of oscillators the interaction will be expressed in terms of the normal coordinates of these oscillators. Emphasizing the fact that $\bar{G}(t)$ is a fluctuating operator with vanishing average it is written (to second order in the normal coordinates) in the form:

$$\bar{G}(t) = \sum_i (K_i(t) - \langle K_i \rangle^F) \cdot Q_i + \sum_i (K_{ii}(t) - \langle K_{ii} \rangle^F) \cdot Q_i^2 + \sum_{i>j} (K_{ij}(t) - \langle K_{ij} \rangle^F) \cdot Q_i Q_j \quad (15)$$

The first two terms in eq.15, to be denoted together by $G_1(t) = \sum_i G_i(t)$ represent the fluctuations of the coupling between the individual oscillators and the bath. For the systems studied in this work this coupling is strong and the fluctuations are large. E.g. the coupling energy can be of the order of kT or about 15% of the energy of $\hbar E^0$ and the fluctuations are not much smaller. Now it is assumed that these fluctuations are very slow with respect to the time scale of interest, which is of the order of 1 psec. The assumption expressed by eq.15 implies that these fluctuations are the same whether the influence of $\hbar G_2(t) = \hbar \sum_{i>j} (K_{ij}(t) - \langle K_{ij} \rangle^F) \cdot Q_i \cdot Q_j$ has been suppressed by isotopic dilution or not.

In view of the supposed slowness of the modulation $\hbar G_1(t)$ it is realistic to consider each system oscillator i as subject to a stationary perturbation $\hbar G_i$ over the time scale of interest. The modulation of $\hbar G_i$ is then represented by a stationary distribution of perturbations. Now the Hamiltonians $\hbar E_i$ of the individual oscillators are redefined to include $\hbar G_i$:

$$\hbar E_i \rightarrow \hbar(E_i + G_i) \quad \hbar G \rightarrow \hbar(G - \sum_i G_i)$$

Obviously this also entails scaling of the normal coordinates Q_i and the interaction constants K_{ij} . The system Hamiltonian $\hbar E = \hbar \sum_i E_i$, which until this stage had a delta function spectrum, is now seen to have a quasicontin-

nuous spectrum. In the following this spectrum is referred to as the unperturbed spectrum. The interaction $\hbar G(t)$ now contains only the fluctuations of the interoscillator coupling:

$$\hbar \bar{G}(t) = \hbar \sum_{i>j} \bar{G}_{ij}(t) = \hbar \sum_{i>j} (K_{ij}(t) - \langle K_{ij} \rangle^F) Q_i Q_j$$

The broadening of the spectrum of $\hbar E$ by very slow modulation is the way in which the concept of inhomogeneous broadening, mentioned in the introduction to this chapter, is introduced here. Inhomogeneous broadening is often invoked in the description of the spectra of hydrogen bonded liquids such as are studied in the present thesis.

By the foregoing description of the system the system Hamiltonian $\hbar E = \hbar \sum_1 E_1$ is now seen to generate a distribution of frequency components of $\phi_{zz}(t)$ in the range of interest. Because Fourier transformation is a linear process all these components contribute additively to $\chi''_{zz}(\omega)$. Conversely one identifies $\int d\alpha P(\alpha) \phi_{zz}^\alpha(t)$ with the experimental autocorrelation function. The frequency distribution function $P(\alpha)$, being the normalised spectrum of $\hbar E$ in the frequency range of interest, is supposed to be known from a reference system lacking the influence of G_2 .

For the sake of clarity a typical experiment may be considered. It consists of the comparison of two solutions of the same solute in a pair of solvents, one of which is a deuterated analog of the other (e.g. solutions in CD_3OH and CD_3OD). The first solvent possesses an absorption band in the neighbourhood of the solute band under study, i.e. $\alpha \simeq \beta$, α and β denoting solute and solvent frequencies respectively. In the second solvent the frequency β is shifted away from α by the isotopic substitution, thereby suppressing the influence of G_2 . (That increasing the difference $\alpha - \beta$ indeed has this effect will be apparent from the results of the theoretical calculations, as was already stated below eq.14). The shape of the solute band in the latter solvent is now supposed to be determined by inhomogeneous broadening only and is consequently taken to be $P(\alpha)$. Because isotopic substitution is the smallest change one can make to a molecule this assumption, which is equivalent to the assumption that the spectrum of $\hbar E$ is the same in both solvents, is considered to be justified.

The interaction Hamiltonian (eq.15) has already been written as a product of system and bath operators. Because it will become clear that the H-bond plays an important part among the bath operators its normal coördinate Q_H will be written explicitly in the expression for $\hbar G_2$ that is used in the calcula-

tion. It is assumed that the hydrogen bond between two molecules exists long enough to execute a significant number of oscillations so that it is reasonable to refer to its normal coordinate. As a matter of fact a normal hydrogen bond vibration executes about 5 cycles per picosecond.

Because compensation for the solvent absorption is assumed to be complete the spectrum is determined by solvent/solute and solute/solute interactions. The latter can be suppressed by dilution and are disregarded in the present theory. In the experimental section of this thesis however some attention will be given to this point.

In terms of normal coordinates the solute/solvent interaction may be written:

$$\hbar\bar{G}_2(t) = \hbar\left\{ \sum_{k,l} C_{kl}(t)Q_kQ_l + \sum_{k,l} C_{kHl}(t)\bar{Q}_H(t)Q_kQ_l \right\} \quad (16)$$

(Throughout the theory the running indices k and l will denote solute and solvent oscillators respectively.)

It is assumed that the terms of $\hbar\bar{G}_2$ are uncorrelated in the sense of the averaging procedure defined by eq.12. In the course of the calculation it will become apparent that often one of the terms of eq.16 dominates. The second term will be used exclusively in the following calculation, because from the result the case in which the first term dominates can be written down immediately.

In summary the above considerations lead us to identify the experimental autocorrelation functions with the following expressions:

$$C^0(t) = N^0 \int d\alpha P(\alpha) \phi_{zz}^{\alpha,0}(t) \quad (17)$$

$$C(t) = N \int d\alpha P(\alpha) \phi_{zz}^{\alpha}(t) = N \int d\alpha P(\alpha) \phi_{zz}^{\alpha,0}(t) \left\langle \left\langle \exp_0 \left\{ i \int_0^t dt' \bar{G}_2^{\times}(t') \right\} \right\rangle \right\rangle \quad (18)$$

$C^0(t)$ and $C(t)$ are the solute transition dipole autocorrelation functions for the band under study for the case that the frequency difference is large and small respectively. The constants N^0 and N normalise the autocorrelation functions to unity at $t=0$.

In order to calculate $C(t)$ from $C^0(t)$ a model for the motions of \vec{M} and G_2 under $\hbar E$ and $\hbar F$ is needed.

Concerning the motion under $\hbar E$ the harmonic approximation is used for all intramolecular oscillators. This implies that each system operator in G_2 , being a product of two normal coordinates, has only four frequency components in its spectral resolution.

The motion of M_z^α under the bath Hamiltonian is considered to be very slow. E.g. the rotational correlation time of a second order Legendre polynomial for methanol (one of the solvents used) is known from N.M.R. to be 4 psec. (ref.6). This implies that the correlation time of the corresponding direction cosine is at least as long, and it is improbable that the solute (the acetate ion) should move faster.

The motion of G_2 under the bath Hamiltonian is now described in terms of a generalised step process (ref.7). Each possible time history $\bar{G}_2(t)$ is considered to be a realisation of the stochastic process:

$$\bar{G}(\xi, t) = \sum_{-\infty}^{\infty} \bar{G}_j(\xi, t) [U(t - t_j(\xi)) - U(t - t_{j+1}(\xi))] \quad ; \quad t_{j+1} > t_j \quad (19)$$

ξ is the stochastic variable

$U(t)$ is the unit step process defined by $U(t) = 0$ if $t < 0$
 $= 1$ if $t \geq 0$

For the sake of clarity first of all some remarks should be made concerning the stochastic variable, because consistent use of this concept obviates unnecessarily loose use of the term "random variable" when treating stochastic processes.

For practical purposes a stochastic process may be defined by an ensemble of its realisations. All realisations in the ensemble are labeled, and this label is the stochastic variable. Choosing a realisation from the ensemble is the same as assigning a value to this variable. It should be stressed that after this choice nothing about the realisation is "random". When treating stochastic processes it is useful to write the stochastic variable explicitly in the expressions to label quantities that are dependent on the choice of realisation. These quantities are usually referred to as the random variables.

A realisation of the process 19 may be visualised by considering one term j from the sum. For $t < t_j$ the term is seen to vanish by the definition of $U(t)$. At $t = t_j$ the first step function becomes 1 and the term j acquires the value $G_j(t)$. At $t = t_{j+1}$ the second step function also becomes 1 and the term j vanishes again. The process $G(t)$ is therefore seen to be described by a succession of values $G_j(t)$, each existing for an interval (t_j, t_{j+1}) .

It will be clear that many processes can be described in terms of this step process. For convenience a very simple picture of the modulation $G_2(t)$ is presented here. It is assumed that each solute molecule is hydrogen bonded

to only one solvent molecule in such a way that their normal coördinates under study interact. Of course additional hydrogen bonds could be envisaged that do not couple these normal coördinates. As long as the oscillators k and l interact through a hydrogen bond the interaction G_{kl} is assumed constant. When the bond is broken G_{kl} vanishes and is replaced by $G_{kl'}$, corresponding to a new hydrogen bond. $G_{kl'}$ now remains constant until the next step and so on. It is assumed that the values G_{kl} are independent in the sense that the probability of G_{kl} having a certain value after a step is not a function of any of the previous values.

The distribution of the time points $t_j(\xi)$ is assumed to be governed by a Poisson counting process with rate λ .

It is seen that the interaction $G_k = \sum_l G_{kl}$ felt by solute oscillator k is a realisation of the process (19).

Of course the physical model for G_k may be elaborated upon while retaining the mathematical model, but this has not been found necessary in this work.

CALCULATION OF THE DIPOLE MOMENT AUTOCORRELATION FUNCTION.

In order to arrive at an expression for $C(t)$ that can be compared with experiment the average $\langle\langle \exp\{i\int_0^t dt' \bar{G}_2^x(t')\} \rangle\rangle$ defined by eq.12 has to be calculated.

Cumulant expansion to second order gives:

$$\langle\langle \exp\{i\int_0^t dt' \bar{G}_2^x(t')\} \rangle\rangle = \exp\{i\int_0^t dt' \langle\langle \bar{G}_2^x(t') \rangle\rangle_c\} - \int_0^t dt' \int_0^{t'} dt'' \langle\langle \bar{G}_2^x(t'') \bar{G}_2^x(t') \rangle\rangle_c \} \quad (20)$$

It can be shown that under the assumptions used in this theory the first order cumulant $\langle\langle \bar{G}_2^x(t') \rangle\rangle_c$ vanishes. In this connection the crucial assumption is that $C_{kl}(t)$, $C_{kHl}(t)$ and $\cos\theta_k(t)$ are uncorrelated and independent of the frequency α .

As a consequence the second order cumulant reduces to:

$$\begin{aligned} \langle\langle \bar{G}_2^x(t'') \bar{G}_2^x(t') \rangle\rangle_c &\equiv \langle\langle \bar{G}_2^x(t'') \bar{G}_2^x(t') \rangle\rangle - \langle\langle \bar{G}_2^x(t'') \rangle\rangle \langle\langle \bar{G}_2^x(t') \rangle\rangle \\ &= \langle\langle \bar{G}_2^x(t'') \bar{G}_2^x(t') \rangle\rangle \end{aligned} \quad (21)$$

Using this result eq.18 may be rewritten to second order:

$$\begin{aligned} C(t) &= N \int d\alpha P(\alpha) \phi_{zz}^{\alpha,0}(t) \cdot \exp\left\{-\int_0^t dt' \int_0^{t'} dt'' \frac{\text{Tr } \rho [M_z^{-\alpha}, [\bar{G}_2(t''), [\bar{G}_2(t'), \bar{M}_z^\alpha(t)]_-]_+}{\text{Tr } \rho [M_z^{-\alpha}, \bar{M}_z^\alpha(t)]_+}\right\} \\ &\equiv N \int d\alpha P(\alpha) \phi_{zz}^{\alpha,0}(t) \cdot F(\alpha, t) \end{aligned} \quad (22)$$

For convenience in notation we first treat the expression:

$$X(\alpha) \equiv \text{Tr } \rho [M_z^{-\alpha}, [\bar{G}_2(t''), [\bar{G}_2(t'), \bar{M}_z^\alpha(t)]_-]_+ \quad (23)$$

$M_z^\alpha(t)$, the component with frequency α from the spectral resolution of $M_z(t)$ with respect to $\hbar E$, is now written as a sum over the corresponding operators of the oscillators forming the system:

$$\bar{M}_z^\alpha(t) = \sum_k \bar{M}_{z,k}^\alpha(t) = \sum_k \cos \theta_k(t) \cdot \left(\frac{\partial \mu}{\partial Q_k} \right)_0 \cdot Q_k^\alpha \quad (24)$$

$\cos\theta_k$ is the direction cosine of the transition dipole moment of oscillator k with respect to a laboratory fixed z -axis.

The interaction Hamiltonian is resolved in the same way:

$$\bar{G}_2(t') = \sum_{k,1} \sum_{\beta,\gamma} C_{kHl}(t') \bar{Q}_H(t') Q_k^\beta Q_l^\gamma e^{i\beta t'} e^{i\gamma t'} \quad (25)$$

Substituting the expressions 24 and 25 eq.23 takes the form:

$$K(\alpha) = \text{Tr } \rho \sum_{k, \dots, p} \sum_{\beta, \dots, \epsilon} \cos \theta_k(o) \cos \theta_p(t) \left(\frac{\partial \mu}{\partial Q_k} \right)_o \cdot \left(\frac{\partial \mu}{\partial Q_p} \right)_o \cdot C_{1Hm}(t'') \cdot C_{nHo}(t') \cdot [Q_k^{-\alpha}, [\bar{Q}_H(t'') Q_1^\beta Q_m^\gamma, [\bar{Q}_H(t') Q_n^\delta Q_o^\epsilon, Q_p^\alpha]_-]_+]_+ e^{i(\beta+\gamma)t''} e^{i(\delta+\epsilon)t'} \quad (26)$$

This expression is simplified considerably by application of the following rules:

- 1) Each commutator should contain the same normal coördinate twice.
- 2) Each normal coördinate should occur an even number of times in each term from 26.
- 3) The sum of the frequencies of the normal coördinate components should vanish. This is a consequence of the assumption expressed by eq.5 (ref.4).
- 4) Terms depending on three normal coördinates are neglected. This means that correlation between more than two oscillators is disregarded.

Using these rules the summations in eq.26 reduce to:

$$K(\alpha) = \text{Tr } \rho \sum_{k, l} \sum_{\beta} \cos \theta_k(o) \cdot \cos \theta_k(t) \cdot \left(\frac{\partial \mu}{\partial Q_k} \right)_o^2 \cdot C_{kHl}(t'') \cdot C_{kHl}(t') \cdot [Q_k^{-\alpha}, [\bar{Q}_H(t'') Q_k^\alpha Q_l^{-\beta}, [\bar{Q}_H(t') Q_k^{-\alpha} Q_l^\beta, Q_k^\alpha]_-]_+]_+ e^{-i(\alpha-\beta)(t'-t'')} \quad (27)$$

By inspection it is seen that from the sum over β only those terms contribute appreciably that make the frequency difference $\alpha-\beta$ as small as possible. This follows from the fact that this frequency appears in the denominator after the time integrations. Because α and β each have two values (ω_k and ω_l respectively) $\alpha-\beta \approx 0$ or $\approx 2\alpha$ depending on the sign of β . This also shows the effect of isotopic dilution, Because α is a solvent frequency in the neighbourhood of the solute frequency α isotopic substitution of the solvent with the effect of shifting β well away from α ensures that no terms from 27 at all contribute to $C(t)$.

Now the commutators are written out and the trace operation is performed over the system coördinates. This averaging consists of two parts. First the vibrational average is taken over an ensemble of solute oscillators with frequency α , and the same operation is performed on an ensemble of solvent oscillators with frequency β . Then the result has to be averaged over the frequency β . Performing the vibrational average gives:

$$K(\alpha) = \text{Tr} \rho \left\langle \sum_{k,l} \cos \theta_k(0) \cos \theta_k(t) \left(\frac{\partial \mu}{\partial Q_k} \right)_0^2 C_{kHl}(t'') \cdot C_{kHl}(t') \cdot \frac{\hbar^3}{8\alpha^2 \beta} \cdot \right. \\ \left. \cdot \coth \frac{\hbar\alpha}{2kT} \cdot \frac{1}{1 - e^{-\frac{\hbar\beta}{kT}}} \left\{ \bar{Q}_H(t'') \bar{Q}_H(t') - \bar{Q}_H(t') \bar{Q}_H(t'') e^{-\frac{\hbar\beta}{kT}} \right\} \cdot e^{-i(\alpha-\beta)(t'-t'')} \right\rangle^\beta$$

The brackets $\langle \quad \rangle^\beta$ indicate that the average over the frequency β has still to be taken. (28)

By the choice of the model the sum over l has only one term for each term of the sum over k . Consequently the summation over l (being the sum over the solvent oscillators interacting with solute oscillator k) can be omitted. The summation over k is now taken outside the averaging brackets. Because after averaging the result is independent of k the sum now consists of identical terms. Therefore performing this sum results in a factor N , the number density of oscillators with frequency α .

In eq.28 only the positive values of β have been retained by the argument below eq.27. Because $\hbar\beta \gg kT$ the second term in braces is now seen to be small and will consequently be neglected in the following.

All quantities moving under $\hbar F$ have been assumed to be independent of α and β . This allows us to average over system and bath variables separately. The average over the frequency β is calculated by assuming a frequency distribution $P(\beta)$ for the solvent oscillators. If we consider the solvent band shape to be determined predominantly by inhomogeneous broadening this band shape can be taken for $P(\beta)$. Considering as an example the COH bending band of CD_3OH this band is found to be fairly accurately represented by a Lorentzian. Therefore the frequency distribution $P(\beta)$ is written:

$$P(\beta) = \frac{1}{\pi} \cdot \frac{\Delta\beta}{\Delta\beta^2 + (\beta - \beta_0)^2}$$

Replacing now the factor $1 - e^{-\frac{\hbar\beta}{kT}}$ in eq.28 by 1 and disregarding the variation of $1/\beta$ over the main part of $P(\beta)$ the integration over β is performed giving:

$$K(\alpha) = N^\alpha \left\langle \cos \theta_k(0) \cdot \cos \theta_k(t) \cdot C_{kHl}(t'') \cdot \bar{Q}_H(t'') \cdot C_{kHl}(t') \cdot \bar{Q}_H(t') \right\rangle \cdot \\ \cdot \left(\frac{\partial \mu}{\partial Q_k} \right)_0^2 \cdot \frac{\hbar^3}{8\alpha^2 \beta_0} \cdot \coth \frac{\hbar\alpha}{2kT} \cdot e^{-i(\alpha-\beta_0)(t'-t'')} \cdot e^{-\Delta\beta(t'-t'')} \quad (30)$$

Now the average over the bath variables has to be taken. Here a complication arises because the expression to be averaged is a function of two stochastic processes. Both $\cos\theta_k(t)$ and $C_{kHI}(t)\bar{Q}(t)$ develop in time under the bath Hamiltonian but certainly not in the same way.

The direction cosine changes by the slow rotation of the solute molecule in the fluctuating potential well formed by its neighbours.

The interaction is modulated by the making and breaking of hydrogen bonds, either by motion of the solute molecule or by changes in the arrangement of the surrounding solvent molecules or both.

Because the rotation is undoubtedly the slowest process, even slow on the time scale of interest, we propose the following picture of the bath.

During 1 psec the direction cosines of all oscillators suffer only minor changes. Therefore we suppose that for each of the histories $\cos\theta_k(0)\cos\theta_k(t)$ an ensemble of realisations of the process $G_2(t)$ can be found in the sample.

This implies that the averages over both processes can be taken separately. In this stage of the theory the rotational autocorrelation function is of no concern because by definition 12 it cancels from the cumulant.

It is now a straightforward matter to calculate the average

$$\langle C_{kHI}(t'')\bar{Q}_H(t'')C_{kHI}(t')\bar{Q}_H(t') \rangle$$

As G_2 is described by a step process we apply the standard technique to average over an ensemble of realisations by writing:

$$\begin{aligned} \langle C_{kHI}(t'')\bar{Q}_H(t'')C_{kHI}(t')\bar{Q}_H(t') \rangle &= E\{C_{kHI}(t'')\bar{Q}_H(t'')C_{kHI}(t')\bar{Q}_H(t') | I\} \cdot P(I) \\ &\quad + E\{C_{kHI}(t'')\bar{Q}_H(t'')C_{kHI}(t')\bar{Q}_H(t') | I^c\} \cdot P(I^c) \quad (31) \end{aligned}$$

$E\{X(0)X(t) | I\}$ is the expectation of the quantity $X(0)X(t)$ if it is known that no step has occurred in the process $X(t)$ during the interval $(0,t)$. $P(I)$ is the probability that no step has occurred.

$E\{X(0)X(t) | I^c\}$ and $P(I^c)$ have the corresponding meaning for the case that a step has occurred.

Because the distribution of the steps has been assumed to be governed by a Poisson process the probability $P(I)$ is known to be $P(I) = \exp\{-\lambda(t' - t'')\}$ where λ is the rate of the process.

By the independence of the process $G_j(\xi)$ in eq.19 the second term in 31 vanishes. The expectation in the first term is just the autocorrelation function of the bath operator $C_{kHI}(t)Q(t)$ over the interval (t'',t') .

By definition this autocorrelation function can be written in terms of its

spectral density $J(\omega)$:

$$\langle C_{\text{KHL}}(t'') \bar{Q}_H(t'') C_{\text{KHL}}(t') \bar{Q}_H(t') | I \rangle = \int_{-\infty}^{\infty} d\omega J(\omega) e^{i\omega(t'-t'')} \quad (32)$$

Now the role of the hydrogen bond becomes clear. The presence of the hydrogen bond energy levels in the bath causes $J(\omega)$ to have peaks at $+\omega_H$ and $-\omega_H$. This implies that the Fourier transform $\int_{-\infty}^{\infty} d\omega J(\omega) e^{i\omega(t'-t'')}$ will oscillate with this frequency. The exact form of $J(\omega)$ is not very important because the time dependence of $F(\alpha, t)$ is seen from eq.30 to be dominated by Δ_β which is of the order 10 psec^{-1} for the systems studied.

Furthermore it is not the object of the present theory to calculate a detailed band shape from the details of molecular motion. Instead it is only attempted to rationalise two experimental parameters, the broadening and the shift of an I.R. band, in terms of a postulated interaction. The purpose of such a theory is to identify the most important factors that cause the effect under study.

Therefore we simply postulate:

$$\int_{-\infty}^{\infty} d\omega J(\omega) e^{i\omega(t'-t'')} = \frac{K^2}{2} \cdot e^{-\lambda'(t'-t'')} \cdot \{ e^{i\omega_0(t'-t'')} + e^{-i\omega_0(t'-t'')} \} \quad (33)$$

Setting $t' = t''$, K^2 is seen to be the variance of the process $C(\xi)Q(\xi)$.

The influence of the bath has now been expressed in a bath correlation time $\Lambda^{-1} = (\lambda + \lambda')^{-1}$ and a variance, together describing the stochastic modulation of the interaction, and a frequency ω_0 to be visualised as an average hydrogen bond frequency.

This represents in mathematical form the physical ideas that fluctuations in the bath cause relaxation of the system and that the hydrogen bond frequency at least partly closes the energy gap between solvent and solute oscillators that would otherwise seriously impede relaxation.

This last point will be discussed in more detail when the explicit form of $C(t)$ has been calculated.

Using eqs.31 and 33 eq.30 finally takes the form:

$$K(\alpha) = N^\alpha \langle \cos \theta_k(0) \cos \theta_k(t) \rangle \cdot \left(\frac{\partial \mu}{\partial Q_{k/0}} \right)^2 \cdot \frac{\hbar^3}{16\alpha^2 \beta_0} \cdot K^2 \cdot \coth \frac{\hbar\alpha}{2kT} \cdot e^{-i(\alpha - \beta_0 - \omega_0)(t'-t'')} \cdot e^{-(\Delta_\beta + \Lambda)(t'-t'')} \quad (34)$$

Here the second term of eq.33 has been omitted because the frequency $\alpha - \beta_0 + \omega_0$ is large so that the corresponding term would give a negligible contribution. Now the result 34 is substituted in $F(\alpha, t)$ defined in eq.22 giving:

$$F(\alpha, t) = \exp\left\{-\int_0^t dt' \int_0^{t'} dt'' \cdot\right.$$

$$\left. N^\alpha \langle \cos \theta_k(o) \cos \theta_k(t) \rangle \cdot \left(\frac{\partial \mu}{\partial Q_k}\right)_o^2 \cdot \frac{\hbar^3}{16\alpha^2 \beta_o} \cdot K^2 \cdot \coth \frac{\hbar \alpha}{2kT} \cdot e^{-i(\alpha - \beta_o - \omega_o)(t' - t'')} \cdot e^{-(\Delta_\beta + \Lambda)(t' - t'')} \right.$$

$$\left. \cdot \text{Tr } \rho [M_z^{-\alpha}, \bar{M}_z^\alpha(t)]_+ \right.$$

(35)

Straightforward calculation yields the following expression for the 0th order autocorrelation function $\phi_{zz}^{\alpha, o}(t)$:

$$\begin{aligned} \phi_{zz}^{\alpha, o}(t) &= \text{Tr } \rho [M_z^{-\alpha}, \bar{M}_z^\alpha(t)]_+ \cdot e^{i\alpha t} = \\ &= N^\alpha \langle \cos \theta_k(o) \cos \theta_k(t) \rangle \cdot \left(\frac{\partial \mu}{\partial Q_k}\right)_o^2 \cdot \frac{\hbar}{2\alpha} \cdot \coth \frac{\hbar \alpha}{2kT} \cdot e^{i\alpha t} \end{aligned} \quad (36)$$

By use of this form eq 35 reduces to:

$$F(\alpha, t) = \exp\left\{-\int_0^t dt' \int_0^{t'} dt'' \cdot \frac{\hbar^2}{8\alpha\beta_o} \cdot K^2 \cdot e^{-i(\alpha - \beta_o - \omega_o)(t' - t'')} \cdot e^{-(\Delta_\beta + \Lambda)(t' - t'')} \right\} \quad (37)$$

Now the time integrations are performed with the result:

$$F(\alpha, t) = \exp\left[-\frac{\hbar^2 K^2}{8\alpha\beta_o} \cdot \left\{ \frac{t}{\Delta_\beta + \Lambda + i(\alpha - \beta_o - \omega_o)} + \frac{e^{-i(\alpha - \beta_o - \omega_o)t} e^{-(\Delta_\beta + \Lambda)t} - 1}{\{\Delta_\beta + \Lambda + i(\alpha - \beta_o - \omega_o)\}^2} \right\} \right] \quad (38)$$

Now it is possible to calculate the average over α in eq.22 which results in the final form for $C(t)$. However, before proceeding it is worthwhile to analyse eq.38 in some detail because all important effects can already be deduced from this formula.

In doing this we anticipate the experimental system with which the theory will be compared by using numerical values taken from this system.

For practical reasons most data have been obtained on solutions of potassium acetate in CD_3OH and CD_3OD . The solute oscillators k are the asymmetric OCO stretching vibrations of the acetate ions, the oscillators l are the COH bending vibrations of the solvent. The corresponding wavenumbers are 1560 cm^{-1} and 1390 cm^{-1} respectively. Δ_β has the value 7.5 psec^{-1} ; the hydrogen bond wavenumber and the bath correlation time are estimated to be 100 cm^{-1} and 0.5 psec respectively. This yields the parameters $\Delta_\beta + \Lambda = 9.5 \text{ psec}^{-1}$ and $\alpha_o - \beta_o - \omega_o \approx 13 \text{ psec}^{-1}$ (see also Chapter V).

For the purpose of illustration the central frequency α_0 of the distribution $P(\alpha)$ is used because this has the greatest weight in the average. It is illustrative to consider first the case of complete resonance, i.e. $\alpha_0 - \beta_0 - \omega_0 = 0$. Then 38 takes the form:

$$F(t) = \exp \left[- \frac{\hbar^2 K^2}{8\alpha_0 \beta_0} \left\{ \frac{t}{\Delta_\beta + \Lambda} + \frac{e^{-(\Delta_\beta + \Lambda)t} - 1}{(\Delta_\beta + \Lambda)^2} \right\} \right] \quad (39)$$

Eq.39 actually describes the hypothetical case in which the solute spectrum is a delta function located at the maximum of the solvent band. As will be shown in the appendix the same form is obtained by substitution of the actual solute band shape in eq.38 while shifting it on the frequency axis so as to make $\alpha_0 - \beta_0 - \omega_0 = 0$, and integrating over α . Therefore eq.39 can be used for the discussion of the resonant case. A situation comparable to this exists for the symmetric OCO stretching band of the acetate ion in CD_3OH . In this case $\alpha_0 - \beta_0 = 0$. As will be discussed in the following this implies that the term hG_2 not containing the hydrogen bond normal coördinate now dominates. Unfortunately this solute band can only be observed qualitatively.

$F(t)$ is now seen to be real, which implies that in the case of resonance no second order shift will be found. Indeed this is observed to be the case.

The second term in the exponent loses its time dependence after 0.2 psec, i.e. when $t \gg (\Delta_\beta + \Lambda)^{-1}$. When on the other hand $t \ll (\Delta_\beta + \Lambda)^{-1}$ $F(t)$ is approximately represented by:

$$F(t) = \exp \left\{ - \frac{\hbar^2 K^2}{8\alpha_0 \beta_0} \cdot \frac{t^2}{2} \right\} \quad (40)$$

On such a short time scale every modulation is necessarily slow. Then we correctly find the Gaussian behaviour characteristic of the slow modulation limit. (ref.8).

For longer times $F(t)$ is an exponentially decaying function of time with the time constant $\frac{\hbar^2 K^2}{8\alpha_0 \beta_0} \cdot \frac{1}{\Delta_\beta + \Lambda}$

If the unperturbed solute absorption band is reasonably well represented by a Lorentzian (as it actually is) it will remain so under the perturbation but with greater width. This is e.g. found to be the case for the symmetric OCO stretch band of acetate ions in CD_3OH . The short time behaviour of $F(t)$ will only cause the far wings of the band to decay faster.

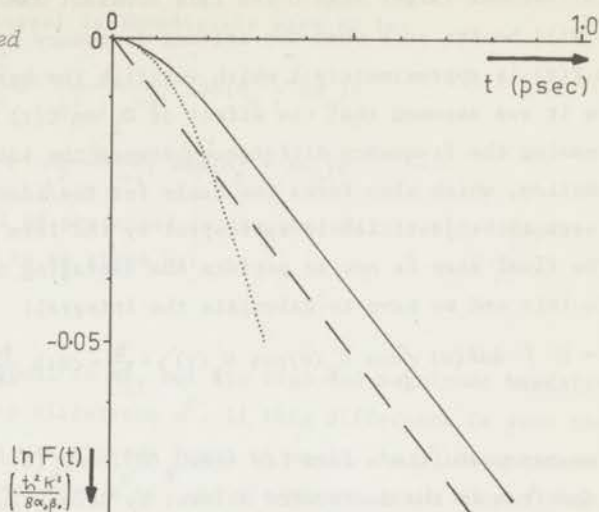
For illustration the time dependence of $F(t)$ (eq.39) is shown in fig. 1.

Fig. 1 $\ln F(t)$ calculated from eq. 39.

Solid line: complete formula

Broken line: $-\frac{t}{\Delta_\beta + \Lambda}$

Dotted line: $-\frac{1}{2}t^2$



Now we consider the more general case in which $\alpha - \beta - \omega_0 \neq 0$.

It is still true that the time dependence of $F(\alpha, t)$ for $t > 0.2$ psec is determined by the first term of the exponent in eq.38. Therefore we limit the discussion to this term; eq.38 then reduces to:

$$F(\alpha, t) = \exp\left\{-\frac{\hbar^2 K^2}{8\alpha\beta_0} \cdot \frac{t}{\Delta_\beta + \Lambda + i(\alpha - \beta_0 - \omega_0)}\right\} \quad (41)$$

Defining for convenience in notation

$$\frac{\hbar^2 K^2}{8\alpha\beta_0} = \sigma^2 \quad \frac{\hbar^2 K^2}{8\alpha_0\beta_0} = \sigma_0^2$$

$$\alpha - \beta_0 - \omega_0 = \omega \quad \alpha_0 - \beta_0 - \omega_0 = \omega^0 \quad \Delta_\beta + \Lambda = \Delta$$

eq.41 can be rewritten:

$$F(\alpha, t) = \exp\left\{-\sigma^2 \frac{t}{\Delta + i\omega}\right\} = \exp\left\{-\sigma^2 \cdot t \cdot \frac{\Delta}{\Delta^2 + \omega^2}\right\} \cdot \exp\left\{i\sigma^2 t \frac{\omega}{\Delta^2 + \omega^2}\right\} \quad (42)$$

$F(\alpha, t)$ is now seen to oscillate with a frequency proportional to σ^2 .

This implies that now the interaction causes a second order shift in addition to the broadening. From 42 it can be seen that the broadening will be less than in the resonant case because the rate constant $\sigma^2 \frac{\Delta}{\Delta^2 + \omega^2}$ is always smaller than $\frac{\sigma^2}{\Delta}$.

However, as long as $|\omega| < \Delta$ the difference is not very large. On the other hand

if $|\omega|$ becomes larger than Δ the rate constant diminishes quickly. This will be the case when the solvent frequency β_0 is shifted by deuteration. Then $F(t)$ is approximately 1 which verifies the hypothesis stated below eq.14. There it was assumed that the effect of G_2 on $C(t)$ would be suppressed by increasing the frequency difference between the interacting oscillators. This assumption, which also forms the basis for the identifications 17 and 18, is now seen to be justified in retrospect by the form of eq.41.

The final step is now to perform the averaging over the solute frequency α . To this end we have to calculate the integral:

$$C(t) = N \int_{\text{band}} d\alpha P(\alpha) \langle \cos \theta_k(0) \cos \theta_k(t) \rangle \cdot \frac{\hbar}{2\alpha} \cdot \coth \frac{\hbar\alpha}{2kT} \cdot \left(\frac{\partial \mu}{\partial Q_k} \right)_0^2 \cdot e^{i\alpha t} \cdot \exp\left\{-\sigma^2 \frac{t}{\Delta + i\omega}\right\} \quad (43)$$

Now we may postulate a form for $\langle \cos \theta_k(0) \cdot \cos \theta_k(t) \rangle$ and generate $P(\alpha)$ from the spectrum in the deuterated solvent by deconvolution. However we may as well neglect the slow motion of $\langle \cos \theta_k(0) \cdot \cos \theta_k(t) \rangle$ relative to the much faster motion of $F(t)$ and of the Fourier transform of $P(\alpha)$. Therefore we identify $P(\alpha)$ with the experimental band shape in the deuterated solvent. Absorbing $\langle \cos \theta_k(0) \cos \theta_k(t) \rangle$ in N eq. 43 takes the form:

$$C(t) = N \int_{\text{band}} d\alpha \frac{\Delta\alpha}{\Delta^2 + (\alpha - \alpha_0)^2} \cdot \frac{\hbar}{2\alpha} \cdot \coth \frac{\hbar\alpha}{2kT} \cdot \left(\frac{\partial \mu}{\partial Q_k} \right)_0^2 e^{i\alpha t} \cdot \exp\left\{-\sigma^2 \frac{t}{\Delta + i\omega}\right\} \quad (44)$$

Because the integral in eq.44 seemed intractable it has been computed numerically for various sets of parameters σ^2 , Δ , and ω^0 .

Because the integrand is only nonvanishing in a relatively small frequency range around the high central frequency α_0 the α -dependence of σ^2 and $\frac{\hbar}{2\alpha} \cdot \coth \frac{\hbar\alpha}{2kT}$ was suppressed in the actual computation by fixing these quantities at their values for $\alpha = \alpha_0$. Furthermore α_0 was chosen as the frequency origin in order to suppress the oscillation at this frequency which would otherwise occur.

Somewhat surprisingly the result of the numerical integration agrees fairly well with the formula which is obtained by suppressing the α -dependence of $F(\alpha, t)$ completely by replacing α with α_0 and integrating analytically:

$$C(t) = N \int_{\text{band}} d\alpha \frac{\Delta\alpha}{\Delta^2 + (\alpha - \alpha_0)^2} \cdot \exp\{-\sigma_0^2 \cdot t\} \cdot \frac{\Delta}{\Delta^2 + \omega_0^2} \cdot e^{i(\alpha + \delta\alpha_0)t} \quad (45)$$

The real part of this integral is immediately seen to be:

$$\begin{aligned}
 C(t) &= e^{-\Delta \alpha \cdot t} \cdot \exp\left\{-\sigma_o^2 \cdot t \cdot \frac{\Delta}{\Delta^2 + \omega_o^2}\right\} \cos(\alpha_o + \delta\alpha_o)t \\
 &= C^o(t) \exp\left\{-\sigma_o^2 \cdot t \cdot \frac{\Delta}{\Delta^2 + \omega_o^2}\right\} \cos(\alpha_o + \delta\alpha_o)t
 \end{aligned}
 \tag{46}$$

The numerical results will be presented in the appendix to this chapter.

The shift $\delta\alpha_o$ is found to be given by:

$$\delta\alpha_o = \sigma_o^2 \frac{\omega_o}{\Delta^2 + \omega_o^2}
 \tag{47}$$

As expected it is proportional to σ_o^2 , but its sign and magnitude are also determined by the frequency difference ω_o . If this difference is zero the shift is seen to vanish as was already found in eq.39. As ω_o is increased the shift goes through a maximum when $\omega_o = \Delta$ and disappears again when ω_o becomes large.

In practice the autocorrelation functions $C(t)$ and $C^o(t)$ are determined by transforming the bands with their respective maxima as the frequency origin. Consequently the factor $\cos(\alpha_o + \delta\alpha_o)t$ does not occur in the experimental functions $C(t)$ and $C^o(t)$.

Therefore the ratio of the experimental autocorrelation functions is found from eq. 46 to be given (for longer times) by:

$$C(t)/C^o(t) = \exp\left\{-\sigma_o^2 \cdot t \cdot \frac{\Delta}{\Delta^2 + \omega_o^2}\right\}
 \tag{48}$$

Eq. 48 shows that this ratio is an exponential function of time while for $t \ll \Delta^{-1}$ a Gaussian part is expected because also in the nonresonant case $F(\alpha, t)$ is Gaussian for $t \ll \Delta^{-1}$. In practice however the short time behaviour of an autocorrelation function cannot be determined with any degree of precision because it is governed by the far wings of the band (ref.1). Therefore also the short time behaviour of the ratio of two such functions cannot be determined dependably. Moreover also the short time behaviour of eq.48 is meaningless because the distribution functions $P(\alpha)$ and $P(\beta)$ have been chosen Lorentzian. This implies that their far wings are physically unrealistic because any real absorption band should decay faster in the wings than a Lorentzian does.

From eq.48 the ratio $C(t)/C^o(t)$ is seen to depend on the parameters σ_o^2 , Δ and ω_o . The shift is (by eq.47) a function of the same quantities. This renders impossible a unique fit with experiment. Fortunately reasonable values for the bath correlation time (e.g. 1 psec) do not appreciably influen-

ce the result by virtue of the large width of the solvent band which yields $\Delta_{\beta} = 7.5 \text{ psec}^{-1}$.

By the arguments presented above it is seen that the short time form of $C(t)/C^0(t)$, which should provide a third datum, cannot be used. The same applies to the value of this ratio for longer times, which is generally different from the value of a pure exponential function with the same time constant (see also fig.1).

It will be clear by now that the treatment presented above applies in the case that $\alpha_0 - \beta_0 - \omega_0$ is the smallest frequency found in the system. Another extreme case that can be treated readily is the case that $\alpha_0 - \beta_0$ is the smallest frequency, i.e. when the solvent and solute bands have nearly the same maximum. It is easy to see that the only modification is that in eqs.44 and 45 ω^0 has the meaning $\omega^0 = \alpha_0 - \beta_0$ and that the bath correlation time Λ^{-1} is changed to λ^{-1} , the reciprocal of the rate of the Poisson modulation (cf. eq.31).

It is also clear that for situations between these extremes the two terms of G_2 cannot be disentangled. Even for the first case the contributions to the bath correlation time, i.e. from the Poisson modulation and from the hydrogen bond spectral density, cannot be separated. Nevertheless in the systems studied in this thesis comparison with experiment will show that satisfactory agreement can be obtained by use of reasonable parameter values. Furthermore the essential role of the hydrogen bond is shown by the fact that the broadening and the shift cannot be simultaneously fitted unless a realistic value for its central frequency ω_0 is assumed. Omitting the hydrogen bond and fitting the broadening e.g. results in a shift that is too large by a factor of 2.5.

A further point to mention is that the solute band shape has also been determined in mixtures of the "normal" solvent and its deuterated analog. In these solutions the broadening was studied as a function of the mole fraction of the normal solvent. In order to adapt the theory to the analysis of these results we have only to modify the summation over l in eq.28. Originally this sum, being the sum over the solvent oscillators coupled to an individual solute oscillator, was considered to have only 1 term and was consequently omitted. If we denote the mole fraction of the normal solvent in the solvent mixture by x_H it is clear that we may still omit this summation if we multiply the expression 30 by x_H . This signifies that only a fraction x_H of the solvent/solute pairs will have the correct frequency matching for G_2 to

have effect.

Then the ratio $C(t)/C^0(t)$ takes the form:

$$C(t)/C^0(t) = \exp\left\{-\sigma_o^2 \cdot t \cdot x_H \frac{\Delta}{\Delta^2 + \omega_o^2}\right\} \quad (49)$$

This implies that the logarithm of this ratio should be a linear function of x_H . The same can be seen to apply for the shift. Both predictions are verified by experiment.

Concerning the value to be used for Δ_β it should be remarked that the COH bending band of CD_3OH is itself strongly broadened by (near-)resonant inter-oscillator coupling. This is of course to be expected because these normal coördinates will certainly be coupled by hydrogen bonds and will therefore interact strongly. On dilution with CD_3OD the half width is found to decrease from 63 cm^{-1} at $x_H = 1$ to 39 cm^{-1} at infinite dilution. It is interesting to note that below $x_H = 0.5$ no shift is found on dilution while the width decreases linearly throughout the range of compositions. Of course the value of 39 cm^{-1} has to be used for Δ_β .

SOME REMARKS CONCERNING CONVERGENCE.

The theory developed in the previous sections is essentially a perturbation expansion, broken off after the second order. Obviously this presents the question if the convergence of the perturbation series is fast enough to justify this. Although the ultimate test of a theory is comparison with experiment it would be more satisfying to have some theoretical justification also.

When designing a theory one attempts to ascertain convergence by a judicious definition of the perturbation in terms of which the desired quantity is to be expanded. In the present work this has been done by expanding in terms of the fluctuation of a specified interaction rather than in the interaction itself. A second important point is the use of the cumulant expansion method instead of the more usual direct expansion of the time dependence of the operator $M(t)$. For the purpose of comparison this latter method is sketched briefly here.

Using the expansion of the time evolution operator $U(t)$:

$$U(t) = U_0(t) \sum_{n=0}^{\infty} (-i)^n \int_0^t dt' \dots \int_0^{t^{(n-1)}} dt^{(n)} \bar{G}(t') \dots \bar{G}(t^{(n)})$$

and the relation $M(t) = U^\dagger(t) \cdot M \cdot U(t)$ the time dependence of $M(t)$ can be expanded:

$$M(t) = \bar{M}(t) + i \int_0^t dt' [\bar{G}(t'), \bar{M}(t)]_- - \int_0^t dt' \int_0^{t'} dt'' [\bar{G}(t''), [\bar{G}(t'), \bar{M}(t)]_-]_- \dots$$

Substitution of this result in the dipole autocorrelation function gives:

$$\begin{aligned} \text{Tr } \rho [M, M(t)]_+ &= \text{Tr } \rho [M, \bar{M}(t)]_+ + i \int_0^t dt' \text{Tr } \rho [M, [\bar{G}(t'), \bar{M}(t)]_-]_+ \\ &\quad - \int_0^t dt' \int_0^{t'} dt'' \text{Tr } \rho [M, [\bar{G}(t''), [\bar{G}(t'), \bar{M}(t)]_-]_-]_+ \dots \end{aligned}$$

This expression is to be compared with the corresponding result of the cumulant expansion method:

$$\begin{aligned} \text{Tr } \rho [M, M(t)]_+ &= \text{Tr } \rho [M, \bar{M}(t)]_+ \cdot \exp \left\{ i \int_0^t dt' \left(\frac{\text{Tr } \rho [M, [\bar{G}(t'), \bar{M}(t)]_-]_+}{\text{Tr } \rho [M, \bar{M}(t)]_+} \right)_c - \right. \\ &\quad \left. - \int_0^t dt' \int_0^{t'} dt'' \left(\frac{\text{Tr } \rho [M, [\bar{G}(t''), [\bar{G}(t'), \bar{M}(t)]_-]_-]_+}{\text{Tr } \rho [M, \bar{M}(t)]_+} \right)_c \dots \right\} \end{aligned}$$

It is easily seen that while the cumulant expansion method gives to second order:

$$C(t)/C^0(t) = \exp(-A \cdot t)$$

the direct method yields:

$$C(t)/C^0(t) = 1 - A \cdot t$$

When $A \cdot t \ll 1$ these expressions are equivalent, but for times $t > A^{-1}$ the direct expansion causes $C(t)$ to become negative, and for $t > 2 \cdot A^{-1}$ it would even be larger in absolute value than $C^0(t)$.

Clearly this is an undesirable situation, even more so since e.g. for the asymmetric OCO stretching band of acetate ions in CD_3OH the quantity A has the value 1.72 psec^{-1} .

Actually one would expect that the effect of a random perturbation with vanishing average and limited correlation time would vanish after some time. This is indeed seen to be a feature of the result of cumulant expansion.

Provided the narrowing condition (vide infra) is met and only the long time behaviour is considered this is even true irrespective of the order to which the cumulant expansion is carried (of course beyond the second). This follows from the asymptotic form for the cumulant function $K(t)$ at long times (ref.8). This function is defined by:

$$\left\langle\left\langle e^{i \int_0^t dt' \bar{G}^x(t')} \right\rangle\right\rangle \equiv e^{K(t)}$$

and can be expanded in the form:

$$K(t) = \sum_1^{\infty} i^n \int_0^t dt' \dots \int_0^{t^{(n-1)}} dt^{(n)} \left\langle\left\langle \bar{G}^x(t^{(n)}) \dots \bar{G}^x(t') \right\rangle\right\rangle_c$$

In the present theory this series was broken off after the second order term.

For $t \gg \tau_c$ this term is given by $-\int_0^t dt' \int_0^{t'} dt'' \left\langle\left\langle \bar{G}^x(t'') \bar{G}^x(t') \right\rangle\right\rangle_c = -\Delta^2 \cdot \tau_c \cdot t$

where τ_c is the correlation time of $G(t)$ and Δ is the r.m.s. amplitude of the modulation. The n^{th} order term has the asymptotic form $O(\Delta^n \tau_c^{n-1}) \cdot t$ when $t \gg n \cdot \tau_c$. Therefore the terms of $K(t)$ omitted by the second order treatment are summed to an error of the order $O\{\Delta \Sigma (\Delta \tau_c)^n\} \cdot t$

When the narrowing condition $\Delta \cdot \tau_c < 1$ is met this sum converges rapidly.

These considerations can now be used to make an order of magnitude estimate of the error introduced by the second order treatment.

It is to be stressed however that since we are interested in the long time behaviour the form of the time dependence (i.e. exponential) is independent

of this error. This is because after a sufficiently long time every term of the cumulant function becomes time-proportional.

This is to be contrasted with the direct expansion method in which higher powers of t come from higher order terms.

A further point is that in the present work cross correlation is neglected (vide rule 4 below eq.26). By the form of G_2 this implies that all odd order cumulants vanish. This causes the leading term of the error sum to vanish.

Using the definition of Δ : $\Delta^2 \equiv \langle\langle G^X(o) G^X(o) \rangle\rangle$ and the experimental value of $\Delta^2 \cdot \tau_c = 1.72 \text{ psec}^{-1}$ we find

$$\Delta = 6.3 \text{ psec}^{-1} \quad \tau_c = 0.04 \text{ psec} \quad \Delta \tau_c = 0.26$$

As $\Delta \cdot \tau_c < 1$ we see that the narrowing condition is met. The error sum is found to predict an error of the order 0.1 psec^{-1} .

Therefore the second order approximation is considered adequate, especially in view of the approximate nature of the model used.

REFERENCES.

1. P.C.M. van Woerkom, thesis Leiden 1974.
2. P.C.M. van Woerkom, J. de Bleijser, M. de Zwart and J.C. Leyte, Chem. Phys. 4, 236 (1974).
3. R. Kubo, J.Ph.Soc.Jap. 12, 570 (1957).
4. R. Kubo and K. Tomita, *ibid.* 9, 888 (1954).
5. R. Kubo, *ibid.* 17, 1100 (1962).
6. H. Versmold and C. Yoon, Ber. Bunseng. 76, 1164 (1972).
7. P.E. Pfeiffer, "Concepts of Probability Theory", ch. 7 (Mcgraw-Hill 1965).
8. R. Kubo in "Fluctuation Relaxation and Resonance in Magnetic Systems" Ter Haar Ed. (Oliver and Boyd, Edinburgh, 1962) p. 23 ff.

APPENDIX. NUMERICAL INTEGRATIONS.

The last step in the calculation presented in the foregoing section is taking the average over the frequency α .

The integral to be performed is given by:

$$C(t) = C(\alpha_0)^{-1} \int_{-\infty}^{\infty} d(\alpha - \alpha_0) \frac{\Delta\alpha}{\Delta^2 + (\alpha - \alpha_0)^2} \cdot e^{i(\alpha - \alpha_0)t} \cdot \exp \left[-\frac{\hbar^2 K^2}{8\alpha\beta_0} \cdot \left\{ \frac{t}{\Delta_\beta + \Lambda + i(\alpha - \beta_0 - \omega_0)} + \frac{e^{-i(\alpha - \beta_0 - \omega_0)t} e^{-(\Delta_\beta + \Lambda)t} - 1}{\{\Delta_\beta + \Lambda + i(\alpha - \beta_0 - \omega_0)\}^2} \right\} \right] \quad (A1)$$

In this expression a factor $\exp(i\alpha_0 t)$ has been omitted in order to suppress the oscillation with the frequency α_0 which would otherwise occur. Omitting this factor is in accordance with the usual practice of transforming an I.R. band with respect to its maximum as the frequency origin.

Evidently $C(t)$ is a complex function and can consequently be written

$$C(t) = CT(t) + i.ST(t) \quad (A2)$$

Defining for convenience of notation the quantities

$$\begin{aligned} A &= \Delta_\alpha & x &= \alpha - \alpha_0 \\ B &= \Delta_\beta + \Lambda & M &= \frac{\hbar^2 K^2}{8\alpha_0 \beta_0} \\ D &= \alpha_0 - \beta_0 - \omega_0 \end{aligned}$$

and the auxiliary functions $RE(t)$ and $IM(t)$:

$$RE(t) = \frac{B \cdot t}{B^2 + (x+D)^2} + \frac{e^{-Bt} [\{B^2 - (x+D)^2\} \cos(x+D)t - 2B(x+D) \sin(x+D)t] - \{B^2 - (x+D)^2\}}{\{B^2 + (x+D)^2\}^2} \quad (A3)$$

$$IM(t) = \frac{(x+D)t}{B^2 + (x+D)^2} + \frac{e^{-Bt} [\{B^2 - (x+D)^2\} \sin(x+D)t + 2B(x+D) \cos(x+D)t] - 2B(x+D)}{\{B^2 + (x+D)^2\}^2} \quad (A4)$$

the functions $CT(t)$ and $ST(t)$ can be written:

$$CT(t) = CT(o)^{-1} \int_{-\alpha_0}^{\infty} dx \frac{A}{A^2 + x^2} \exp\{-M \cdot RE(t)\} \cdot \cos\{x \cdot t - M \cdot IM(t)\} \quad (A5)$$

$$ST(t) = CT(o)^{-1} \int_{-\alpha_0}^{\infty} dx \frac{A}{A^2 + x^2} \exp\{-M \cdot RE(t)\} \cdot \sin\{x \cdot t - M \cdot IM(t)\} \quad (A6)$$

The simplified expression 44 has also been integrated. Using the same symbols as above this expression takes the form:

$$C(t) = C(o)^{-1} \int_{-\alpha_0}^{\infty} dx \frac{A}{A^2 + x^2} e^{ixt} \exp\left\{-M \cdot \frac{t}{B + i(x+D)}\right\} \quad (A7)$$

Splitting A7 into real and imaginary parts gives:

$$CT(t) = CT(o)^{-1} \int_{-\alpha_0}^{\infty} dx \frac{A}{A^2 + x^2} \cdot \exp\left\{-M \cdot t \cdot \frac{B}{B^2 + (x+D)^2}\right\} \cdot \cos\left\{x + M \cdot \frac{x+D}{B^2 + (x+D)^2}\right\} \cdot t \quad (A8)$$

$$ST(t) = CT(o)^{-1} \int_{-\alpha_0}^{\infty} dx \frac{A}{A^2 + x^2} \cdot \exp\left\{-M \cdot t \cdot \frac{B}{B^2 + (x+D)^2}\right\} \cdot \sin\left\{x + M \cdot \frac{x+D}{B^2 + (x+D)^2}\right\} \cdot t \quad (A9)$$

The integrals A5, A6, A8 and A9 have been computed on an IBM 370/158 computer. The parameters to be varied are M (representing the mean squared amplitude of the modulation of G_2), B and D .

The resonant case is obtained by setting $D = 0$. As was already stated in the preceding section $\alpha - \beta_0$ is then the smallest frequency to be found in the system. This causes the term in G_2 without the hydrogen bond normal coordinate to dominate. The definition of the quantity B then changes to $B = \Delta_\beta + \lambda$

Only the integrals A5 and A8, being the real part of $C(t)$, will be treated in detail.

While the complete electric moment autocorrelation function is real (and even in t) the function $C(t)$ will generally be complex. This is because it represents only the part of the autocorrelation function corresponding to the band under study determined by positive frequencies.

In the present theory calculation of $\Phi_{ZZ}^\alpha(t)$ is sufficient to describe the influence of G_2 on the shape of the absorption band. This is a consequence of the assumption underlying this work (and practically all I.R. work as well) viz. that an absorption band can be described separately from all other bands in the spectrum. This assumption implies that a component, corresponding to

the band under study, can be separated uniquely from the electric moment autocorrelation function of the sample.

Then the symmetry properties of the autocorrelation function imply that the part $\phi_{ZZ}^{\alpha}(t)$ of this component, governed by positive frequencies, is the complex conjugate of the negative frequency part $\phi_{ZZ}^{-\alpha}(t)$.

Because under this assumption the admittance in the (positive) frequency range of the band under study is determined by:

$$\chi''(\omega) = \frac{\omega}{4E_{\beta}(\omega)} \int_{-\infty}^{\infty} dt e^{-i\omega t} \phi_{ZZ}^{\alpha}(t) \quad ; \quad \omega \text{ around } \alpha_0 \quad (\text{A10})$$

inversion of this Fourier transform, shifting the frequency origin and equating real and imaginary parts gives the identification:

$$\text{CT}(t) = N \cdot \text{Re} \left(\phi_{ZZ}^{\alpha}(t) \right) = \int_{\text{band}} d\omega I(\omega) \cos \omega t \quad (\text{A11})$$

$$\text{ST}(t) = N \cdot \text{Im} \left(\phi_{ZZ}^{\alpha}(t) \right) = \int_{\text{band}} d\omega I(\omega) \sin \omega t \quad (\text{A12})$$

The RHS of eq.A11 is the normalised cosine transform of the experimental band shape $I(\omega)$, calculated with respect to its maximum as the frequency origin. This function displays the broadening effect of G_2 . The asymmetry of the band shape is expressed in the sine transform and consequently given in terms of G_2 by eq.A12.

In the case that $C(t)$ is real this sine transform vanishes and the band is consequently symmetric. This situation is encountered in the case of the symmetric OCO stretching band of the acetate ion which does broaden by interaction with the COH bending of CD_3OH but remains symmetric in shape, contrary to the as. stretch. The reason for this is that the sym. stretching band happens to have practically the same central frequency as the COH bending band of the solvent.

All cosine transforms $\text{CT}(t)$ computed numerically are found to have the form

$$\text{CT}(t) = \exp\left(-\frac{t}{\tau}\right) \cos(\delta \cdot t) \quad (\text{A13})$$

Both for A5 and A8 the time constant is found to be approximately:

$$\frac{1}{\tau} \approx M \frac{B}{B^2 + D^2} \quad (\text{A14})$$

The shift found from eq.A8 is given by:

$$\delta = M \frac{D}{B^2 + D^2} \quad (\text{A15})$$

while the shifts from eq.A5 appear to be smaller than this by approximately 20%.

SOME RESULTS OF THE NUMERICAL INTEGRATIONS.

When eq.A5 is integrated using values for the parameters B, D and M giving approximate agreement with experiment the resulting $C(t)$ is found to be non-exponential. Actually it is seen to become negative after 0.7 psec as is shown by fig. A1 curve a. This curve has been calculated with the values $B = 9 \text{ psec}^{-1}$, $D = 13 \text{ psec}^{-1}$ and $M = 40 \text{ psec}^{-2}$. If the frequency origin is shifted by 1.70 psec^{-1} , corresponding to a shift of $+9 \text{ cm}^{-1}$, curve b is obtained. This function is exponential as is shown by fig. A2 (a). In this figure the function $\ln C(t) - \ln C^0(t)$ is plotted vs. time. This function directly shows the effect of G_2 and is therefore a convenient measure to be used in the discussion.

Fig. A1. $C(t)$ calculated from eq. A5 with the parameters $B = 9 \text{ psec}^{-1}$, $D = 13 \text{ psec}^{-1}$ and $M = 40 \text{ psec}^{-2}$.

Curve a: shift = 0

Curve b: shift = $+9 \text{ cm}^{-1}$.

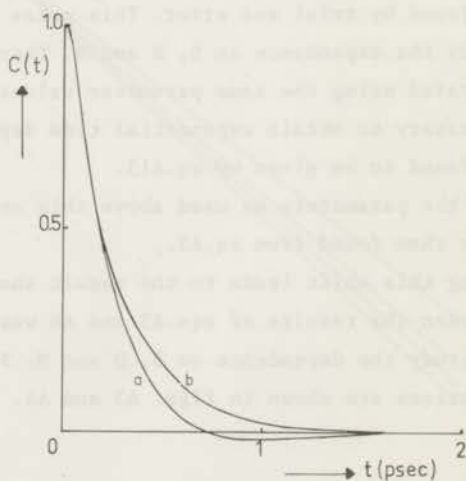


Fig. A2. $\ln C(t) - \ln C^0(t)$
 calculated from eq. A5
 (curve a) and eq. A8 (curve
 b). Parameter values:

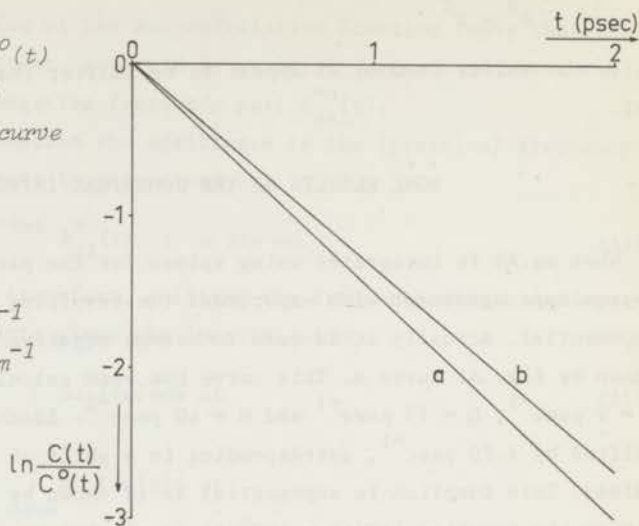
$$B = 9 \text{ psec}^{-1}$$

$$D = 13 \text{ psec}^{-1}$$

$$M = 40 \text{ psec}^{-2}$$

$$\text{Shift for eq A5: } +9 \text{ cm}^{-1}$$

$$\text{Shift for eq A8: } +11 \text{ cm}^{-1}$$



The shift necessary to obtain the best exponential time dependence had to be found by trial and error. This makes eq.A5 unattractive as an object to study the dependence on B, D and M. Therefore the simplified eq.A8 was integrated using the same parameter values. Also in this case a shift is necessary to obtain exponential time dependence, but for eq.A8 this shift is found to be given by eq.A15.

For the parameters as used above this corresponds with $+11 \text{ cm}^{-1}$ i.e. 20% more than found from eq.A5.

Using this shift leads to the result shown by fig.A2 (b). The agreement between the results of eqs.A5 and A8 was considered sufficient to use A8 to study the dependence on B, D and M. Some of the results of these calculations are shown in figs. A3 and A4.

Fig. A3. $\ln C(t) - \ln C^0(t)$ calculated from eq A8 as a function of D . From top to bottom: $D = 16, 15, 14, 13$.

Other parameters:

$$B = 9 \text{ psec}^{-1}$$

$$M = 40 \text{ psec}^{-2}$$

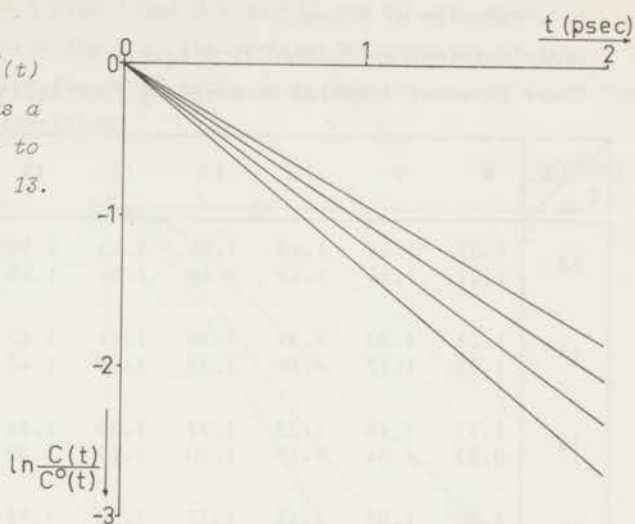
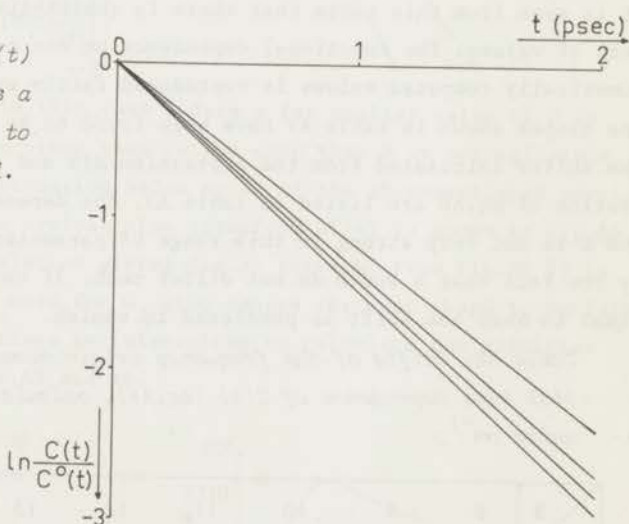


Fig. A4. $\ln C(t) - \ln C^0(t)$ calculated from eq A8 as a function of B . From top to bottom: $B = 8, 9, 10, 11$.

Other parameters:

$$D = 13 \text{ psec}^{-1}$$

$$M = 40 \text{ psec}^{-2}$$



In table A1 the slopes of these lines are compared to the quantity $M \cdot \frac{B}{B^2 + D^2}$. This quantity is presented in the upper entries. The lower entries are calculated from the results of the numerical integration of eq.A8.

Table A1. Absolute values of the slope of $\ln C(t) - \ln C^D(t)$ (psec^{-1}) as a function of B and D.

Upper entries: calculated from eq.A14.

Lower entries: computed numerically from eq.A8.

B \ D	8	9	10	11	12	13	14	15	16
13	1.37 1.21	1.44 1.34	1.48 1.43	1.52 1.49	1.53 1.53	1.54 1.55	1.53 1.57	1.52 1.57	1.51 1.56
14	1.23 1.05	1.30 1.17	1.35 1.26	1.39 1.33	1.41 1.38	1.42 1.42	1.43 1.44	1.43 1.45	1.42 1.45
15	1.11 0.93	1.18 1.04	1.23 1.13	1.27 1.20	1.30 1.25	1.32 1.29	1.33 1.32	1.33 1.34	1.33 1.35
16	1.00 0.83	1.07 0.92	1.12 1.01	1.17 1.08	1.20 1.14	1.22 1.18	1.24 1.22	1.25 1.24	1.25 1.25

It is seen from this table that there is qualitative agreement between both sets of values. The functional dependence on the parameters B and D of the numerically computed values is reproduced fairly well.

The slopes shown in table A1 have been found to be proportional to M.

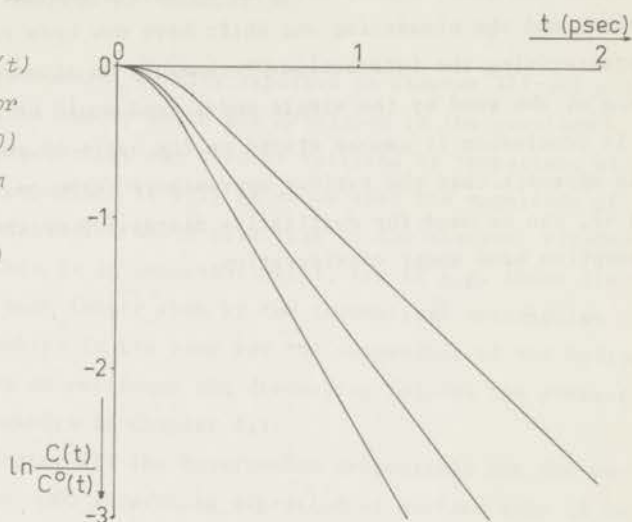
The shifts calculated from the expression A15 and used in the numerical integration of eq.A8 are listed in table A2. The dependence of the shift on B and D is not very strong in this range of parameter values, but this is caused by the fact that B and D do not differ much. If on the other hand D is set equal to zero the shift is predicted to vanish.

Table A2. Shifts of the frequency origin necessary to obtain exponential time dependence of $C(t)$ (eq.A8), calculated from eq.A15; units cm^{-1} .

B \ D	8	9	10	11	12	13	14	15	16
13	11.8	10.8	10.2	9.5	8.8	8.2	7.6	7.0	6.5
14	11.4	10.6	10.1	9.4	8.7	8.1	7.6	7.1	6.6
15	10.9	10.4	9.8	9.2	8.6	8.1	7.6	7.1	6.6
16	10.6	10.1	9.5	9.0	8.5	8.0	7.5	7.1	6.6

This is also found on integrating eq.A5 using this value for D. The results of this computation for $B = 9 \text{ psec}^{-1}$ and $M = 10, 15$ and 20 are shown in fig.A5. By comparing this with fig.1 of the section "Calculation of the Dipole Moment autocorrelation Function" it is seen that the use of eq.39 for qualitative discussion is justified.

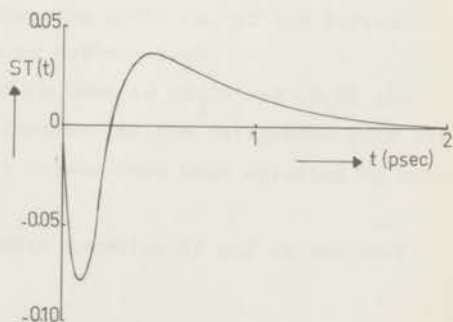
Fig. A5. $\ln C(t) - \ln C^0(t)$ calculated from eq A5 for the resonant case ($D = 0$) as a function of M . From top to bottom:
 $M = 10, 15, 20.$ (psec^{-2})
 $B = 9 \text{ psec}^{-1}$



A point to notice is that in this case indeed a far smaller value of M is necessary to obtain a given slope than in the case that D is nonnegligible. This is in line with the discussion below eq.42 of the aforementioned section.

For illustration only a typical sine transform $ST(t)$ is shown in fig.A6. It corresponds to the calculation giving fig.A1 curve b. From fig.A6 it is anticipated that the model used for G_2 also causes the band shape to deviate from symmetry. It would perhaps be interesting to calculate the predicted band shape by inverting eqs.A5 and A6.

Fig. A6. $ST(t)$ calculated from eq. A5 with the parameters $B = 9 \text{ psec}^{-1}$
 $D = 13 \text{ psec}^{-1}$
 $M = 40 \text{ psec}^{-2}$
 $\text{Shift} = +9 \text{ cm}^{-1}$.



However, this would necessitate the computation of far more values for $CT(t)$ and $ST(t)$ to obtain a sufficient number of points for the inverse transformation. To save programming and cpu time this has so far not been done. Moreover it is doubted if this additional work would provide additional insight. The goal of this study is to assess the main effect of the interaction, and the broadening and shift have now been expressed in the parameters characterising the interaction. Presumably an attempt to describe the complete shape of the band by the simple model used would be pushing the model too far.

In conclusion it can be stated on the basis of the results presented in this appendix that the various approximate formulae, especially eqs. 39, 46 and 47, can be used for qualitative discussion of the effect of G_2 on the absorption band under consideration.

CHAPTER V. DISCUSSION.

In this chapter the experimental results reported in Chapter III are considered with reference to the theory which was developed in the previous chapter. The theoretical predictions can then be verified by comparison with experiment. By numerical comparison it will be shown that the magnitude of the fluctuations of the interaction which give rise to the observed broadening is not unduly large. This is an important point, for if e.g. those fluctuations were found to be much larger than kT the theoretical description would of course not be tenable. In the same way the importance of the hydrogen bond will be seen. For ease of reference the discussion follows the presentation of the experimental results in Chapter III.

In the first part of Chapter III the interaction responsible for the enhanced relaxation of the $\nu_{\text{as.OCO}}$ stretching vibration of acetate ions in methanol was identified. It was shown that the additional relaxation is caused by coupling with the ν_{COH} bending vibration of the solvent. Now it is possible to assess the importance of the hydrogen bond between solvent and solute molecules in this respect. It has already been stated that the hydrogen bond frequency is needed to close, at least partly, the frequency gap of 180 cm^{-1} between the solvent and solute oscillators.

From eq.47 of the preceding chapter, which relates the shift of this frequency gap, it is seen that this gap is not completely bridged, for in that case no shift would be found. On the other hand disregarding the hydrogen bond frequency leads to the situation that either the shift $\delta\alpha_0$ or the increase of the relaxation rate τ^{-1} can be reproduced but not both.

Confining the attention to solutions of CH_3COOK in CD_3OH and CD_3OD the experimental values of the shift and the increase of the relaxation rate are 10 cm^{-1} and 1.7 psec^{-1} respectively. These values have been obtained by extrapolation to zero concentration.

For the purpose of discussion the approximate formulae 47 and 48 are used:

$$\delta\alpha_0 = \tau^2 \frac{\omega^0}{\Delta^2 + \omega^0{}^2}$$

$$\ln \frac{C(t)}{C^0(t)} = -\frac{t}{\tau} = -\sigma^2 \frac{\Delta}{\Delta^2 + \omega^0{}^2}$$

Disregarding the hydrogen bond gives the parameters $\omega^0 = 180 \text{ cm}^{-1} = 33.8 \text{ psec}^{-1}$ and $\Delta = 9 \text{ psec}^{-1}$. The latter value is obtained by estimating the reciprocal of the correlation time of $G_2(t)$ to be 1.5 psec^{-1} . This choice will be commented upon in the following.

Fitting the increase in relaxation rate yields the value 231 psec^{-2} for σ^2 . This in turn gives a shift of $6.4 \text{ psec}^{-1} = 34 \text{ cm}^{-1}$.

On the other hand fitting the shift gives for σ^2 the value 68 psec^{-2} which predicts an increase of τ^{-1} by 0.5 psec^{-1} .

These results show that when fitting τ^{-1} the large value of σ^2 necessary to overcome the effect of the frequency difference forces the shift to an excessively large value, while when fitting the shift σ^2 is insufficiently large to reproduce the experimental increase of τ^{-1} .

From eqs.47 and 48 it is seen that in order to fit the broadening and the shift simultaneously the following equations must be satisfied:

$$\text{For the shift: } 1.88 = \sigma^2 \frac{\omega^0}{\Delta^2 + \omega^0}$$

$$\text{For the broadening: } 1.7 = \sigma^2 \frac{\Delta}{\Delta^2 + \omega^0}$$

Clearly these relations imply $\omega^0 = 1.1 \Delta$

It will now be shown that from the infinitely many solutions reasonable values can be chosen.

The parameter Δ was defined by:

$$\Delta = \Delta_\beta + \Delta = \Delta_\beta + \lambda' + \lambda$$

The solvent band width is experimentally found to be $\Delta_\beta = 7.5 \text{ psec}^{-1}$. The parameter λ , the rate of the Poisson modulation of $G_2(t)$, can be taken to be the reciprocal of the lifetime of a hydrogen bond, which is generally assumed to be of the order of 1 psec . The correlation time $1/\lambda'$ corresponding with the spectral density of the modulation is assumed to be of the same order. Therefore Δ has been estimated to be 9 psec^{-1} . It is however seen that Δ is dominated by Δ_β so that the parameters λ' and λ can be varied considerably without materially influencing the final result.

By the relation $\omega^0 = 1.1\Delta$ ω^0 is found to be $\omega^0 = 10 \text{ psec}^{-1}$.

The assumption that the frequency gap is reduced to this value by the hydrogen bond frequency leads for this frequency to the value $\omega_0 = 23.8 \text{ psec}^{-1} = 127 \text{ cm}^{-1}$, which is a reasonable value.

The mean squared fluctuation of the interaction energy is then found to be

34.2 psec⁻². This means that the interaction G_2 has a r.m.s. fluctuation of $5.85 \text{ psec}^{-1} = 31 \text{ cm}^{-1}$. This is to be compared with kT which is approximately 210 cm^{-1} at room temperature.

We regard the above considerations as compelling evidence for the crucial role of the hydrogen bond, especially in view of the reasonable values found for the quantities ω_0 and σ^2 . This is to be contrasted with the large discrepancies which occur if the hydrogen bond is disregarded.

From eqs.47 and 48 it is seen that in the resonant case the shift should vanish while the broadening should be enhanced. This is clearly borne out by fig.1 which shows both OCO stretching bands of the acetate ion in CD_3OD and CD_3OH . While for technical reasons the sym. band cannot be accurately measured in CD_3OH the broadening certainly is large, and the band is not shifted. While the as. band broadens from 22.5 to 37.5 cm^{-1} the width of the sym. band is seen to increase from 24.5 to 62 cm^{-1} .

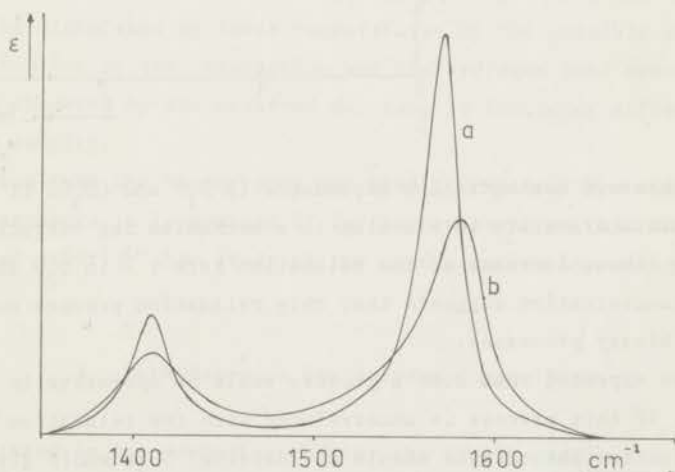
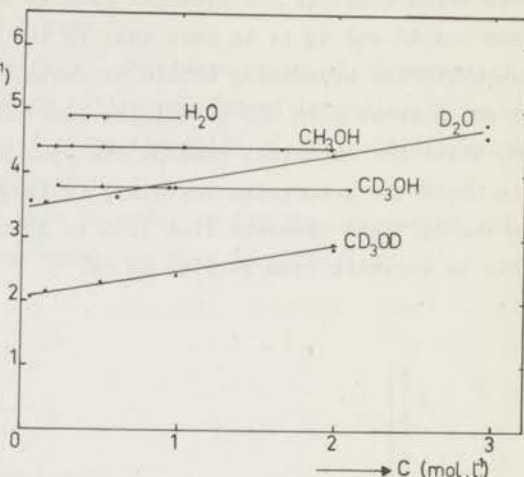


Fig. 1. Spectrum of the OCO stretching vibrations of CH_3COOK in CD_3OD (a) and in CD_3OH (b).

1. Concentration Dependence.

Section 1 of Chapter III (part 2) presents the concentration dependence of τ^{-1} of the as. OCO stretching band of CH_3COOK in various solvents. The results are summarised in fig.2.

Fig. 2. Concentration dependence of the correlation time of the as. OCO stretching band of CH_3COOK in various solvents.



From the observed concentration dependence in D_2O and CD_3OD it is concluded that acetate/acetate interaction is a mechanism for vibrational relaxation. The linear increase of the relaxation rate τ^{-1} in D_2O and CD_3OD with solute concentration suggests that this relaxation process consists of uncorrelated binary processes.

It would be expected that such a process would be operative in the other solvents too. If this process is uncorrelated with the relaxation by solute/solvent interaction the effects should be additive. This would give rise to the same concentration dependence, which is however not observed. The only reasonable way to explain the lack of concentration dependence in CD_3OH , CH_3OH and H_2O therefore seems to be the assumption that both processes are negatively correlated, crosscorrelation offsetting the solute/solute relaxation

Another point is the magnitude of the concentration dependence in CD_3OD and D_2O . Tentative calculations using transition dipole/transition dipole interaction indicate very short distances of closest approach, actually corresponding to collisions. It is not yet clear if this is reasonable.

The above considerations indicate that further research on this topic is necessary. This will be the subject of future work.

2. Temperature Dependence.

While the theoretical results do not explicitly indicate temperature dependence of τ^{-1} and $\delta\alpha_0$, these quantities are in principle temperature dependent mainly by the implicit temperature dependence of the widths and positions of the respective absorption bands.

Experimentally these bands have been found to be only weakly temperature sensitive, and therefore no strong temperature dependence of τ^{-1} and $\delta\alpha_0$ is expected.

Experimentally no temperature dependence has been found, which supports the above discussion. It is concluded that the effects influencing temperature dependence are small and mutually compensating. While the relaxation rate could be diminished at lower temperatures by the possible diminishing of the fluctuation of the interaction and the hydrogen bond spectral density, it could be enhanced by the observed decrease in frequency difference and increase in density.

Considering that the theory does not predict explicitly a significant temperature dependence it is doubted if further research on this topic should have a higher priority than study of the concentration dependence.

3. Dependence on the solvent Composition.

As was stated in the preceding chapter the theory predicts a linear dependence of τ^{-1} on x_H in CD_3OH/CD_3OD mixtures. By the same arguments the shift can also be seen to be a linear function of x_H . These predictions depend essentially on the assumption that the interaction in different solvent/solute oscillator pairs is uncorrelated.

These predictions are seen to be completely verified by experiment. The measurements have been performed on solutions with the same concentration which was chosen as low as practicable in order to obviate possible concentration dependent effects. The COH bending band of CD_3OH in CD_3OD is also dependent on x_H as is to be expected. On dilution this band is narrowed consi-

derably. At mole fractions below 0.5 no shift is found as is expected because the interaction is between oscillators with the same frequency. At high concentrations the description in terms of uncorrelated pairwise interactions presumably breaks down and the theoretical conclusions no longer hold. It has not yet been attempted to devise a theory capable of describing the entire mole fraction range.

4. Influence of some Cations.

Intuitively little effect of the cation on τ^{-1} is expected, except perhaps on the concentration dependence. The latter could e.g. involve ion pairs, the stability of which could be dependent on the cation.

It has been found that no change of τ^{-1} is produced by substitution of Na^+ for K^+ , and that τ^{-1} shows a small increase when Li^+ is the cation. Preliminary measurements on CH_3COOLi in CD_3OD show that in this case the concentration dependence does not differ significantly from that in CH_3COOK .

The cupric ion completely changes the behaviour of the acetate ions. The first point to notice is that the as. OCO stretching band shifts from 1570 to 1626 cm^{-1} . This considerable shift is explained by the fact that Cu^{++} forms a complex with two acetate ions and that consequently the electronic structure of these ions will be altered, with a concomitant change in the vibrational spectrum.

The second effect is that the as. OCO stretching band is much narrower than for CH_3COOK , and that the influence of deuteration of the solvent is much reduced. This is explained by the consideration that the acetate ions undoubtedly are bound to the cupric ions by the carboxylate group. This would screen this group from interaction with the solvent. Likewise it is conceivable that the cupric ion screens the two acetate ions from each other, especially when a square planar arrangement is assumed. It should be noted however that even if the two acetate ions in the complex exchange a vibrational quantum this would not necessarily lead to appreciable relaxation if the complex is stable over a time span of some picoseconds.

5. Influence of the presence of other compounds in the solutions.

No effect was found of saturation of solutions of CH_3COOK in D_2O and CD_3OD with KBr . These solvents were chosen in order to find a possible influence of spectroscopically inert ions on the acetate/acetate interaction.

It has been found that this interaction, which gives rise to the concentration dependence, is influenced by the presence of acetic acid in the solution. Preliminary measurements on CH_3COOLi in CD_3OD in the presence of CD_3COOD show that the concentration dependence of τ^{-1} becomes significantly steeper with increasing concentration of the acid. This study is presently under progress and therefore it will not be treated further here.

Addition of carbon tetrachloride to solutions of CH_3COOK in CH_3OH has no effect on τ^{-1} irrespective of the volume ratio of CCl_4 to CH_3OH . This ratio has been made as high as 10 to 1.

This finding could be regarded as an indication that the interaction which gives rise to the additional relaxation is operative at short range. However due caution should be exercised because nothing definite is known concerning the structure (or even the stability) of such solutions.

Conclusion.

The agreement obtained between experiment and the theoretical description as treated in the foregoing sections is considered to provide ample support for the hypotheses forming the basis of the theory. Comparison of different solvent/solute pairs shows satisfactory agreement of the dependence of τ^{-1} on the frequency difference with the theoretical prediction. Additional evidence is provided by the shifts. The theory predicts that the sign of the shift is governed by the sign of the frequency difference between the interacting oscillators. Indeed the ν_{OCO} stretching band of the acetate ion is shifted from 1570 to 1580 cm^{-1} by the ν_{COH} bending of CD_3OH at 1390 cm^{-1} , while it is shifted from 1560 to 1554 cm^{-1} by the ν_{HOH} bending of H_2O at 1640 cm^{-1} . The corresponding band of the CCl_3COO^- ion is shifted from 1665 to 1680 cm^{-1} comparing solutions in D_2O and H_2O respectively. In all cases the band is "repelled" by the interacting solvent band, as is expected.

Scope for further work

Undoubtedly the most intriguing question posed by the results of the present study is the explanation of the concentration dependence. Both the absence of concentration dependence of τ^{-1} in H_2O , CD_3OH and CH_3OH and the magnitude of the concentration dependence in D_2O and CD_3OD cannot yet be explained. It is also not known if the fact that the concentration dependence in D_2O and CD_3OD is the same is accidental or not.

Possibility N.M.R. relaxation studies on ^{23}Na could provide information on ion pair formation. Also a N.M.R. study of the microdynamics of the acetate ion could be valuable.

Another point that is the subject of future work is the concentration dependence of the COH bending band of CD_3OH in CD_3OD , especially at high mole fractions.

SAMENVATTING

In dit proefschrift wordt een onderzoek beschreven naar intermoleculaire vibratierelaxatie in vloeistoffen waarin waterstofbrug binding optreedt. Deze relaxatie is bestudeerd door vergelijking van de I.R. bandvorm van de asymmetrische OCO rek absorptieband van CH_3COOK in CD_3OH en CD_3OD . Ook aan een aantal vergelijkbare systemen is dit verschijnsel geobserveerd. Aangevoerd wordt dat in het bovengenoemde geval de relaxatie wordt veroorzaakt door wisselwerking tussen de as. OCO rekvibratie van de opgeloste stof (bij 1570 cm^{-1}) en de COH buigvibratie van de oplosmiddelmoleculen (bij 1390 cm^{-1}). In de oplossing in CD_3OD heeft deze wisselwerking geen effect omdat door de deuterering deze vibratie ongeveer 200 cm^{-1} naar lagere golfgetallen verschuift. Hierdoor wordt het frequentieverschil tussen de wisselwerkende oscillatoren te groot, zoals theoretisch wordt aangetoond. Tevens wordt aangetoond dat de grootte van het effect, ondanks het relatief grote frequentieverschil van 180 cm^{-1} , verklaard kan worden doordat de frequentie van de H-brug dit verschil ten dele overbrugt.

Theoretisch is gevonden dat de grootte van het effect, dat zich uit in een aanzienlijke bandverbreding, afhangt van de breedte van de twee absorptiebanden, het frequentieverschil, de frequentie van de H-brugvibraties en in mindere mate van de spectrale dichtheid daarvan. De optredende 2^e orde verschuiving wordt theoretisch in dezelfde grootheden uitgedrukt.

Intermoleculaire vibratierelaxatie wordt ook waargenomen in CD_3OH d.m.v. een verdunningsreeks in CD_3OD . In dit geval wordt de relaxatie veroorzaakt door wisselwerking tussen identieke oscillatoren.

Resonante wisselwerking is eveneens waargenomen door de concentratieafhankelijkheid van de correlatietijd van de as. OCO rek absorptieband van CH_3COOK in CD_3OD . Vibratierelaxatie wordt in dit geval veroorzaakt door wisselwerking tussen de acetaationen onderling. Opvallend is dat dit effect niet wordt waargenomen in oplossingen in CD_3OH ; hierin is de correlatietijd onafhankelijk van de acetaatconcentratie. Dit doet vermoeden dat de $\text{CH}_3\text{COO}^- / \text{CD}_3\text{OH}$ en $\text{CH}_3\text{COO}^- / \text{CH}_3\text{COO}^-$ wisselwerkingen negatief gecorreleerd zijn.

Dit is het onderwerp van verder onderzoek.

Temperatuurafhankelijkheid van enig belang is niet gevonden, hetgeen op grond van de theorie is te verwachten.

De theoretische beschrijving zoals die in dit proefschrift wordt gegeven wordt bevredigend geacht op grond van de goede overeenkomst tussen de experimentele resultaten en de theoretische voorspellingen. Met name het belang van de waterstofbrug voor vibratierelaxatie door niet-resonante wisselwerking wordt als duidelijk aangetoond beschouwd.

Op verzoek van de Faculteit der Wiskunde en Natuurwetenschappen volgt hier een kort overzicht van mijn academische studie.

Na het behalen van het diploma Gymnasium- β aan het St. Franciscuscollege te Rotterdam in juni 1961 werd in hetzelfde jaar de studie in de scheikunde te Leiden begonnen. Het kandidaatsexamen, letter F, werd afgelegd in februari 1965. De doctoraalstudie met als hoofdvak fysische chemie, bijvak theoretische anorganische chemie en derde richting heterogene katalyse stond onder leiding van de hoogleraren Dr. M. Mandel en Dr. W.M.H. Sachtler en de lectoren Dr. J.C. Leyte en Dr. W.J.A. Maaskant. Het doctoraalexamen werd afgelegd in januari 1969.

Hierna werd het onderzoek begonnen dat in dit proefschrift wordt beschreven. Na in de periode van november 1963 tot augustus 1967 als studentassistent verbonden te zijn geweest aan verschillende practica kwam ik in februari 1969 als doctoraalassistent in dienst bij het propaedeutisch chemisch practicum. In februari 1970 volgde benoeming tot hoofdassistent, in februari 1971 tot wetenschappelijk medewerker en in februari 1973 tot wetenschappelijk medewerker I.

Gaarne wil ik hier mijn dank betuigen aan allen die tot het tot stand komen van dit proefschrift hebben bijgedragen. In de eerste plaats dient vermeld te worden dat zonder de zeer vele discussies met mijn promotor Dr. J.C. Leyte en met Dr. P.C.M. van Woerkom de theorie in dit proefschrift niet ontwikkeld had kunnen worden.

Drs. H.S. Kielman komt mijn dank toe voor de belangrijke bijdragen die hij aan het onderzoek heeft geleverd tijdens zijn doctoraalstudie.

Bijzondere dank wil ik betuigen aan de heer D. van Duijn, wiens grote geduld en buitengewone bekwaamheid vele moeilijke metingen mogelijk hebben gemaakt.

Verder dank ik mevr. E.M.J. Rijsbergen en mej. L.H. Zuiderweg voor de bijdragen die zij hebben geleverd aan de vormgeving van dit proefschrift.

The first part of the report deals with the general situation of the country and the progress of the work done during the year. It is followed by a detailed account of the various projects and the results achieved. The report concludes with a summary of the work done and a list of the names of the persons who have taken part in it.

The second part of the report deals with the financial situation of the country and the progress of the work done during the year. It is followed by a detailed account of the various projects and the results achieved. The report concludes with a summary of the work done and a list of the names of the persons who have taken part in it.

